SLAC-PUB-176
ITP-200

# PERIPHERAL PROCESSES*

A. C. Hearn

Institute of Theoretical Physics, Department of Physics
Stanford University, Stanford, California

and

S. D. Drell

Stanford Linear Accelerator Center
Stanford University, Stanford, California

[To be published as Chapter 9 of the book High Energy Physics (Academic Press)]

*Work supported in part by the U. S. Atomic Energy Commission and in part by the U. S. Air Force through Air Force Office of Scientific Research Contract AF 49(638)-1389.

# I. INTRODUCTION

The concept of peripheralism and the range of its applications have been extended considerably in the last few years. In its original form it was a method for extrapolating to pole terms arising from single particle exchange contributions in transition amplitudes. Although these poles are often found close by, they are never within the physical region, and so an accurate procedure for extrapolating from experimental points to the nearest lying pole is required. One hoped to learn from this the coupling parameters or unstable particle cross-sections appearing as residues at the poles.

As an extension of this idea it was next suggested that one choose particular processes and very limited kinematic conditions so that some particular, well defined class of Feynman graphs will have unusually small energy denominators. In the analysis of the corresponding cross sections it is assumed that these graphs, generally with single particle exchange poles near the physical region, dominate over all others. In this manner several channels are isolated from among the full wealth of strongly interacting channels and approximate theoretical predictions can be presented for experimental testing. Although this is a rather primitive approximation scheme it is more attractive than a weak coupling perturbation expansion in powers of the strength of the interaction among pions and nucleons and offers the possibility of relating different experiments to each other. In this spirit a number of calculations were performed and the successes of the predicted relations with experiment, though far from quantitative or uniform, were sufficiently compelling to

trigger a series of more refined analyses attempting to supply some of the more important ingredients missing in the first approximation. These efforts have developed recently into a major program of detailed analyses of the corrections due to the possibility of absorption into the numerous competing open channels that deplete the amplitude in the channel under study. Many promising results have been achieved in this way, and quantitative fits to spectra, angular distributions, and spin correlations have been achieved for a number of interactions.

With this most recent development the emphasis of peripheralism has switched from the search for approximate relations between various experiments and from the prediction of gross qualitative features to a program of detailed analysis. Perhaps the collisions of strongly coupled particles are too rich with detailed information on the nature of their interactions to be analyzed theoretically in full detail. But we may have here a rather valuable phenomenology for many processes. As we shall see very little of the original "peripheralism" is still in evidence at this stage. However, along with many successes, serious deficiencies will be found and remain unsolved by theory.

Our review will proceed chronologically and will describe this evolution in the saga of peripheral processes.

## II. EARLY DEVELOPMENTS

The forward pion-nucleon dispersion relations play a unique role in strong interaction physics, presenting an exact relation between experimental quantities. Equation (II.1), for example, is an exact relation between $T^-(\omega)$, the difference between the $\pi^-p$ and $\pi^+p$ forward scattering amplitudes at energy $\omega$, and $\sigma^{\pi^+p}(\omega') - \sigma^{\pi^-p}(\omega')$, the difference of their total cross sections (Goldberger, 1955).

$$T^-(\omega) = \frac{-4f^2\omega}{\omega^2 - \left[\mu^2/2M\right]^2} + \frac{\omega}{2\pi^2}\int_\mu^\infty \frac{d\omega'\sqrt{\omega'^2-\mu^2}}{\omega'^2-\omega^2-i\epsilon}\left[\sigma^{\pi^+p}(\omega') - \sigma^{\pi^-p}(\omega')\right] \qquad (II.1)$$

They are related in Eq. (II.1) to the pion nucleon coupling constant $f^2$ which appears in the residue at the pole in the forward scattering amplitude for single nucleon exchange in the energy or $\omega$ channel as illustrated in Fig. 1. By extrapolating the scattering amplitude below the threshold for physical scattering, $\omega_t = \mu$, the pion mass, to the pole at $\omega = \mu^2/2M$, a value of $f^2 \approx 0.08$ is found, namely

$$\lim_{\omega \to \mu^2/2M}\left\{\frac{\omega^2 - \left[\mu^2/2M\right]^2}{-4\omega}\ \mathrm{Re}\ T^-(\omega)\right\} = f^2 \qquad (II.2)$$

Once this pole was successfully isolated and its residue, or coupling parameter, accurately measured, it became of prime importance to identify other processes also containing this pole term and to attempt to isolate and measure its residue by similar extrapolation procedures. Chew (1958) proposed the study of elastic nucleon-nucleon scattering at high energies and suitably restricted kinematics with just this purpose in mind. In this case there is a pion exchange pole as illustrated in Fig. 2

appearing in the momentum transfer channel. It contributes a term to the scattering cross section for unpolarized nucleons of the form

$$\frac{d\sigma}{dt} = \frac{R(t)}{p_{inc}^2 (t - \mu^2)^2} \tag{II.3}$$

where $p_{inc}^2$ is the laboratory 3-momentum at the incident proton and where t is the invariant momentum transfer, i.e. $t = (p_1 - p_1')^2$ in terms of the kinematics shown in Fig. 2. R(t) is a momentum transfer dependent factor free of singularities in the neighborhood of the pole, and can be expanded in power series about $t = \mu^2$ within a circle of radius $3\mu^2$, which extends into the physical region $t \leq 0$. At the pole, R(t) is just the product of $f^2$ and known kinematical factors arising from isotopic spin considerations and the p-wave coupling of pseudoscalar mesons to nucleons. In particular, if we concentrate on charge exchange neutron-proton scattering, as is convenient in order to avoid interference in the analysis from both Coulomb effects and the forward diffraction peak for elastic channels, the amplitude in Fig. 2 may be written as

$$T = i(\sqrt{2}\, g)^2 \frac{\left[\bar{u}(p_2' s_2')\, \gamma_5\, u(p_2 s_2)\right] \left[\bar{u}(p_1' s_1')\, \gamma_5\, u(p_1 s_1)\right]}{t - \mu^2} F(t) \tag{II.4}$$

Upon squaring this amplitude, averaging over initial and summing over final spins, the differential cross-section for the process may be written as

$$\frac{d\sigma}{dt} = \frac{4\pi f^2}{\mu^2 p_{inc}^2} \left|F(t)\right|^2 \frac{t^2}{(t - \mu^2)^2} \tag{II.5}$$

where

$$f^2 \equiv \frac{(g\,\mu/2M)^2}{4\pi}$$

and

$$F(0) \simeq F(\mu^2) \equiv 1 \tag{II.6}$$

The normalized "form factor" F(t) includes all corrections to the pion propagator and vertex functions and becomes unity at the pole as defined. The numerator factor $t^2$ arises from the p-wave pion-nucleon coupling. We can also write Eq. (II.5) in terms of the center-of-mass momentum p and the scattering angle (backward for exchange scattering) $\theta$ through the relation

$$t - \mu^2 = -\,2|p|^2 \left[1 + \mu^2/2|p|^2 - \cos\theta\right] \tag{II.7}$$

and extrapolate to the pole at $\cos\theta = 1 + \mu^2/2|p|^2$ by studying the cross-section as a function of angle at fixed center-of-mass momentum. The aim here is to establish that the pion-nucleon coupling constant "measured" by this extrapolation is the same as was found in the forward pion-nucleon amplitude, Eq. (II.2).

A very high degree of accuracy has been achieved by these analyses and the pion nucleon constant as determined by both methods agrees to several percent [Hamilton and Woolcock (1963), Chamberlain (1960), Ashmore et al (1962)] . The extrapolation interval for the forward $\pi$N dispersion analysis is $\mu - (\mu^2/2M) \approx 130$ MeV from the physical

threshold at $\omega_t = \mu$, where $T(\omega)$ develops an imaginary part at the onset of the unitarity or right-hand cut in the energy, or $\omega$, plane. The extrapolation in nucleon-nucleon scattering may be over a very small interval in cos $\theta$ if we are working at a large momentum so that $\mu/p \ll 1$. Also other singularities corresponding to two or more pion exchange are further removed from the physical region as shown in Fig. 3. The branch point at the onset of additional singularities occurs at $t = 4\mu^2$ or the square of the minimum mass of a two pion state.

However the extrapolation to the pole in this case has been very difficult to accomplish with high accuracy, the reason for this originating from the p-wave character of the coupling of pions of odd intrinsic parity to nucleons. This means that the pole term Eq. (II.5) to which we are extrapolating vanishes at the edge of the physical region as $t \to 0$, corresponding to the very peripheral collisions with zero momentum transfer and large impact parameters. For such collisions the velocity of the exchanged pion and hence its p-wave absorption amplitude vanishes. In fact Eq. (II.5) shows that the pole term goes through a second order zero at $t = 0$ on its way to the pole. Since its contribution to the observed cross section is negligible it is no wonder that it is very difficult to isolate this term.

The foregoing discussion shows clearly that quantitative meaning can be attached to the pole analysis for one-pion exchange only if small energy denominators are joined by large numerator functions. We therefore turn our attention to processes with reasonably large amplitudes in the peripheral limit. Consider for example, the cross-section for

$$\pi + p \to \pi + \pi + p$$

in the vicinity of the pion pole shown in Fig. 4. This study was first proposed by Goebel (1958) and by Chew and Low (1959) as a method for obtaining information about the $\pi\pi$ scattering amplitude which occurs at the vertex B, and which cannot be measured directly. The residue at the pion exchange pole at $t = \mu^2$ in this process has the form

$$R = C\, f^2\, \sigma_{\pi\pi} , \qquad (II.8)$$

where C is a known kinematical factor. So given the value of f, the pion-nucleon coupling constant determined from the earlier extrapolation, we may determine a value for $\sigma_{\pi\pi}$ by extrapolation to this pole. The value we obtain for $\sigma_{\pi\pi}$ is not, of course, the physical pion-pion cross-section as one of the pions is necessarily off the mass-shell in the determination. Presumably however it is approximately equal to the physical cross-section. This assumption that $\sigma_{\pi\pi}$ does not change appreciably in an energy interval of $\sim$ 140 MeV as the mass of one of the external pion lines is extrapolated to $\leq 0$ is similar to that made in Eq. (II.6) in relating the pion-nucleon coupling constants as determined from $\pi$N and NN scattering pole terms. Without this assumption of a smooth behavior and of slow variation over the energy range $\sim \mu \simeq$ 140 MeV, no quantitative analyses relating different cross-sections of the strongly interacting particles to each other can be achieved.

Our remarks apply with equal validity to many other processes where similar unmeasurable cross-sections occur, e.g. extrapolation of $\pi p(\pi)\ K\bar{K}p$

gives $\sigma_{\pi\pi K\bar{K}}$, and extrapolation of $Kp(\pi)\ K\pi p$ gives $\sigma_{K\pi K\pi}$, where our notation for a process indicates the exchanged particle in parentheses.

The next extension of the peripheral idea again rests on the importance of the near-lying pole. If this pole is close by, then it is reasonable that the peripheral diagram should dominate in the physical region nearest the pole. This assumption is motivated theoretically by the fact that the energy denominator is very small in this region and the transition amplitude falls off rapidly with increasing momentum transfer. If the exchanged particle is very light, then the effect is obviously even more marked, and so should work best with pion exchange. Experimentally, too, a forward peaking is observed in many processes and can be attributed to large impact parameter collisions, such as the peripheral model provides. In this manner we can see that the cross-section for $\pi p \rightarrow 2\pi p$ should have a maximum at low momentum transfer if the $\pi\pi$ interaction is not negligibly small. A larger cross-section and perhaps simpler experiment now suggests itself for determining unstable particle cross-sections as illustrated in Fig. 5, where now only the two high-energy pions emerging in the forward direction within an angle $\theta \sim \mu/k$ of the incident pion of energy k are detected (Drell, 1961). The exchanged virtual pion is allowed to plough into the target nucleon and to initiate reactions to any possible final states. In this way the full pion-nucleon cross-section is developed at vertex A in place of the small amplitude for absorbing a slow pion, and so the physical value of $\sigma_{\pi\pi}$ may be determined from studying the forward cross-section of the production process.

Since the simple peripheral model offers such a straightforward method of calculation it is easy to carry the calculations far into the physical region away from the single particle exchange pole, and compare the results with experiment. It is not surprising that such a simple picture cannot reproduce the experimental data far from the pole, because we can now no longer regard the exchanged particle as quasi-real as we could in the forward region. "Off-mass-shell" corrections arising from the virtual nature of the exchanged particle have to be made and other particle exchange graphs considered as well. This realization triggered a whole series of calculations which include form factors corrections to the vertices but we shall leave the discussion of these until the next Section.

Up till now we have discussed extensions of the peripheral idea without subjecting the model to any serious test of its validity. In fact, even if one allows some arbitrary form factor dependence at the vertices, the assumption of single particle exchange in a process makes very simple and unique predictions about the angular distribution of the scattered particles. These predictions are supplementary to any made about momentum and energy distributions and can form the basis for tests of the one-pion-exchange (OPE) model as pointed out by Treiman and Yang (1962) and Goldhaber (1964). For example, in the particular case illustrated in Fig. 4, it is clear that the spin zero meson exchanged cannot communicate information between the vertices A and B about the direction of the momentum transfer but only about its magnitude. From this it follows that there can be no correlation between the production plane of the pions in the rest system

of the incident pion and the scattering plane of the nucleons. In other words, in terms of the angles illustrated in Fig. 6, the distribution of the produced pions is independent of the azimuthal angle $\varphi$ and therefore has the form

$$W(\theta,\varphi) = \sum a_n \cos^n \theta \qquad \text{(II.9)}$$

If furthermore the production occurs through a single resonance channel of well defined spin and parity as in Fig. 7, the decay distribution is limited to the form

$$W(\theta,\varphi) = \sum_{n=1}^{N} a_{2n} \cos^{2n} \theta \ , \qquad \text{(II.10)}$$

where N is the spin of the resonant state.

In this particular case as well, if we observe the decay distribution in the rest frame of the $\rho$, there can be no component of spin along the incident pion direction (which, in this frame, is parallel to the momentum direction of the exchanged pion). This requires that the $\rho$ have only longitudinal polarization along the incident pion direction and implies that the decay distribution vanish at $\theta = 90^\circ$ and thus have the form

$$W(\theta,\varphi) = \cos^2 \theta \qquad \text{(II.11)}$$

Similar but more complicated arguments can be made when the exchanged particle has non-zero spin. [Stodolsky and Sakurai (1963), Gottfried and Jackson (1964b)]. These will be discussed in Section IV.

So far, the only extension of the simple peripheral model we have considered has been the addition of form factors at the vertices. Another possibility is that some form of interaction between the target and scatterer may occur in addition to the peripheral exchange. In particular, in the high energy region (above 1 GeV) one expects that elastic diffraction scattering will occur in the initial and final states as shown in Fig. 8. Even if this initial and final state scattering does not cause any spin or helicity change in the amplitudes, it is now possible for information on the direction of the momentum transfer to be carried between the target and the scatterer, and so our previous predictions on decay correlations will no longer be valid. We shall show that observed deviations in angular and t distributions from the simple peripheral picture can be attributed either to form factors or to such initial and final state interactions. Changes in the decay distributions, however, can only be explained by rescattering corrections.

Statements can also be made about the energy dependence of the cross-section but so far there has been little theoretical progress on this point as will be most apparent in Section V.

## III. THE PERIPHERAL MODEL WITH FORM FACTORS

We now consider in more detail the application of the peripheral mechanism to inelastic processes. The approach we use is to look for particular Feynman graphs which have very small energy denominators in the kinematical region we are considering. We turn again to the reaction

$$\pi + N \rightarrow \pi + \pi + N .$$

In addition to the formation of nucleon isobars in the scattering channel, which contribute calculable amounts over known energy and momentum ranges, there are poles in the matrix elements coming from peripheral exchanges. Of these, the pion is the lightest state and has a pole lying very near to the physical region which is expected to influence the reaction most.

Direct experimental evidence for this assumption is provided by looking at the angular distributions for $\pi^- + p \rightarrow \pi^- + \pi^+ + n$ at 1.59 GeV/C as shown in Fig. 9. We see there a marked forward peaking which suggests the dominance of a long range interaction mechanism such as single pion exchange.

According to the usual Feynman rules, the amplitude for such a diagram has the form

$$T = V_A V_B / (t - \mu^2) , \qquad \text{(III.1)}$$

where t as before is the negative squared four-momentum transfer in the production channel and $V_A$, $V_B$ are the contributions from the vertices A and B in Fig. 4. These vertices can be expressed generally as form factors

depending on t multiplying the spinor factors as computed for the lowest order Feynman graph. $V_A$ and $V_B$ contain all contributions from diagrams which contribute to the vertex "blobs" of Fig. 4, but do not include initial and final state interactions of the form shown in Fig. 8, which we shall discuss later.

At the $\pi NN$ vertex, a spectral form can be written for the form factor. We define a form factor F(t) by

$$V_{\pi NN} = \bar{u}(p_2)\ \gamma_5\ g\ F(t)\ u(p_1) \tag{III.2}$$

where $\bar{u}$ and u are final and initial Dirac spinors for the nucleons, g is the rationalized $\pi N$ coupling constant ($g^2/4\pi = 14.4$) and $F(\mu^2) = 1$. F(t) then satisfies a dispersion relation of the form

$$F(t) = 1 + \frac{(t - \mu^2)}{\pi} \int_{9\mu^2}^{\infty} \frac{\sigma(t')\ dt'}{(t' - \mu^2)(t' - t)} \tag{III.3}$$

The weight function in the spectral integral has a threshold at $t = 9\mu^2$, the square of the least massive state to which a pion couples, and may assume negative as well as positive values, so no general statements about F(t) can be made. F(t) is a dispersion-theoretic form factor as distinct from a Dyson irreducible vertex function and thus includes corrections to the virtual pion propagator.

There are analogous "form factor" corrections at the four particle $\pi\pi$ scattering vertex which depend upon the distance of the exchanged pion from the mass shell at $t = \mu^2$. These unknown form factors depend only on the momentum transfer. On one hand they must be introduced phenomenologically, since accurate calculation is impossible. On the other hand, as they do not

depend on the energy of the reaction, the adequacy of an approach which keeps only the class of diagrams that correspond to one pion exchange can be readily tested. The energy dependence of the cross-sections at fixed t is the same as the Born approximation result from lowest order perturbation theory, and the various angular decay tests, such as the Treiman-Yang test (1962) can be applied.

This form factor approach has been applied most extensively in a series of papers describing work initiated by Ferrari and Selleri and a review of the fits with references complete up until 1962 is given in Ferrari and Selleri (1962). A more recent discussion with references may be found in Selleri (1964). In our expression Eq. (III.1) for the matrix element, the unknown part appears as a product of form factors, G(t) and it is this product which is fitted, using a Clementel-Villi (1956) form:

$$G(t) = A - B\mu^2/(t - C\mu^2) \ , \qquad \text{(III.4)}$$

the constants A, B and C being found from experiment. By an analysis of the processes

$$p + p \rightarrow p + n + \pi^+$$

$$p + p \rightarrow p + p + \pi^o$$

Ferrari and Selleri (1963) found the following values for the constants:

$$A = 0.28, \quad B = 3.42, \quad C = 5.75 \ , \qquad \text{(III.5)}$$

which gave a quantitative fit to the processes up to about 1 GeV. A significant feature of the analysis was that the same product of form factors could also reproduce the cross-sections for other one pion exchange

reactions such as $\pi N \to \rho N$, $\pi N \to \rho N^*$, $KN \to K^* N^*$, $N\bar{N} \to N^* \bar{N}^*$. In other words, once the product was determined phenomenologically for one such reaction, the theory was determined for a whole class of reactions over an appreciable range of energies.

In spite of this success, there are several serious shortcomings to the form factor approach. First, on a purely theoretical level, there is the question of trying to relate the parameters Eq. (III.5) to "reasonable" or "physically simple" approximations to the dispersion integrals. For example, can one understand the t dependence of G(t) near t = 0, or is this dependence too rapid? Since G(t) represents a product of form factors at the two vertices of Fig. 4 divided by a propagator form factor, there is however no direct way of relating the constant C to the known physical singularities.

Secondly, as we shall see later, the observed angular correlations of final state particles cannot be reproduced by a simple form factor modification of the single particle exchange amplitude.

In addition we have limited ourselves so far to reactions below 1 or 2 GeV. If we attempt to take the form factor approach to higher energies, even for the simplest case of one pion exchange, further adjustments to the model are necessary in order to reduce the excessively high predictions of the model for large momentum transfer. Several authors have treated the exchanged particle as a Regge pole. [Islam (1963), Islam and Pinon (1963) Shaw and Wong (1963) Gottfried and Jackson (1964a)] This has the required effect of reducing the high energy cross-section, but introduces more parameters into a fit which already has a certain amount of arbitrariness.

Another approach is that of Amaldi and Selleri (1964), who expressed the product of form factors G(t) as a sum of two terms of the Clementel-Villi type; one to give a rapid decrease at small momentum transfers and the other with a long tail to fit the data at relatively large momentum transfers, viz:

$$G(t) = \frac{0.72}{1 - (t - \mu^2)/4.73\,\mu^2} + \frac{0.28}{1 + \left[(t - \mu^2)/32\,\mu^2\right]^2} \qquad \text{(III.6)}$$

Again this seems a rather ad hoc procedure, and so leads one to believe that some other mechanism not yet taken into account may be operating.

Finally, fits with the form factor model are far from satisfactory for processes involving vector exchange. Not only must the value of C in Eq. (III.5) be much smaller (in fact smaller than $\mu^2$) if a Clementel-Villi form factor is used [Daudin et al, (1963)], but the energy dependence of the reactions cannot be satisfactorily fitted for processes which are dominated by an exchange with spin greater than zero.

For these reasons, various authors have suggested that initial and final state interactions must be considered in order to understand the peripheral mechanism correctly. This approach, which we discuss in the next section, suggests that the form factor model is inadequate for dealing with anything but medium energy phenomena, and that, even there, it may only be one of several alternative ways of parametrizing the true physical situation.

## IV. THE PERIPHERAL MODEL WITH ABSORPTION

### A. Derivation of the Model

We have seen in the previous section that in spite of the success of the form factor approach to inelastic peripheral processes at medium energies, the technique needs such serious modification at higher energies that its whole validity must be questioned. The peripheral mechanism was suggested by the obvious dominance of the forward peaking in all reactions we have studied so far. However, a naive calculation with the unmodified model is unable to account for all the observed peaking, implying a mechanism more peripheral than we have discussed so far. The forward peaked cross-sections suggest a long range mechanism, but it is well known that the pole approximation has appreciable contribution from the low partial waves; the S-wave, in particular, being strong enough in many cases to violate the limit imposed by unitarity. At the same time, at very high energies, the production process under consideration may constitute only a small part of the total cross-section. For example, in an experiment involving 2.08 GeV/c $\pi^+$ incident on hydrogen, some of the cross-sections measured were [James and Kraybill (1966)]

| | | | |
|---|---|---|---|
| $\pi^+ p \to \pi^+ p\, \pi^o$ | 5.62 ± 0.20 mb | $\to p\, \rho^+$ | 2.19 ± 0.19 mb |
| | | $\to N^*\, \pi^o$ | 0.62 ± 0.08 mb |
| $\to \pi^+ p\, \pi^+ \pi^-$ | 3.03 ± 0.07 mb | $\to \pi^+ p\, \rho^o$ | 0.91 ± 0.10 mb |
| $\to \pi^+ p\, \pi^+ \pi^- \pi^o$ | 2.29 ± 0.07 mb | $\to \pi^+ p\, \omega^o$ | 1.81 ± 0.19 mb |
| | | $\to \pi^+ p\, \eta^o$ | 0.74 ± 0.14 mb |
| $\to \pi^+ \pi^+ \pi^+ \pi^- n$ | 0.22 ± 0.02 mb | | |

Intuitively, one would expect the more complex interactions to be initiated by collisions involving low partial waves, and conversely this would imply that the low partial wave interactions are less likely to contribute to the process under discussion. In other words, the existence of many competing open channels should imply a reduction in the low partial wave interaction amplitudes to any one channel while leaving the higher partial waves essentially unchanged. This would require a reduction of the production cross-section and modify the angular distributions, producing as we shall see an enhancement of the forward angle cross-section as given by experiment.

The idea that such final state interactions must be included in order to describe the peripheral mechanism correctly is not new. Baker and Blankenbecler (1962) considered the coupling of many open channels by dispersion theory and found strong absorption in the low partial waves. A simpler approach was used by Sopkovich (1962 a,b) to calculate angular distributions for $p\bar{p} \to \Lambda\bar{\Lambda}$. He used the Glauber (1959) high energy approximation for the production amplitude, distorting the amplitude by an optical potential to describe the initial and final state scattering. The results of this calculation were however dependent on the parameters used to describe the optical potential.

An even simpler model to explain the observed diffraction effect in the same process (Fig. 10) was proposed by Dar et al (1964). This was essentially Fraunhofer diffraction scattering from an illuminated ring. If the ring has radius R, then one can write

$$\frac{d\sigma}{d\Omega} = A\left(1 + \frac{k_i}{k_f} \cos\theta\right)^2 \left[J_o(q\,R)\right]^2, \qquad \text{(IV.1)}$$

where A is a normalization factor, $J_o$ is the cylindical Bessel function and $\underset{\sim}{q} = \underset{\sim}{k}_f - \underset{\sim}{k}_i$, the difference between final and initial momenta. The parameters A and R were adjusted to fit the data. Obviously this is a gross oversimplification of the true physical situation, but it gives a very simple qualitative explanation of a possible mechanism. A more convincing approach along similar lines is to assume that below some fixed angular momentum L all partial wave projections of the single particle exchange matrix element are zero. This forms the basis of a model of Bugg (1963) which was used to fit n-p charge exchange scattering. The same idea is discussed in more generality by Dar and Tobocman (1964), and was used by Dar (1964) to fit a wide variety of processes involving pseudoscalar and vector exchange. These analyses were made using the impact parameter representation of the scattering amplitude rather than partial waves, which is appropriate when one is dealing with high energies and small angles and so a large number of partial waves are contributing. In this case, we can replace the partial wave sum

$$T_{fi} = \sum_{\ell=0}^{\infty} (\ell + \tfrac{1}{2})\, T_\ell(k)\, P_\ell(\cos\theta) \qquad \text{(IV.2)}$$

by an integral

$$T_{fi} = \int_0^\infty b\, db\, T(k,b)\, J_o(\Delta\, b), \qquad \text{(IV.3)}$$

where k is the incident 3-momentum in the center-of-mass, $kb = \ell + 1/2$, $\Delta = \sqrt{-t}$ is the magnitude of the invariant 4-momentum transfer and $J_o$ is

the Bessel function of zeroth order. We have also made use of the small angle approximation

$$P_\ell(\cos\theta) \simeq J_o\left[(2\ell + 1)\sin(\theta/2)\right] \tag{IV.4}$$

in deriving Eq. (IV.3).

We see that the integration variable b may be identified with the classical impact parameter, leading to a simple physical interpretation of the representation.

The impact parameter representation of the single particle exchange scattering amplitude is given by

$$A = (M^2 - t)^{-1} = \int_o^\infty b\, db\, K_o(Mb)\, J_o(\Delta b), \tag{IV.5}$$

where $K_o$ is the zeroth order modified Bessel function of the second kind. If we now assume that the integrand is zero below a fixed radius R, we have

$$\begin{aligned} A_{\text{modified}} &= \int_R^\infty b\, db\, K_o(Mb)\, J_o(\Delta b) \\ &= MR(M^2 - t)^{-1}\left\{K_1(MR)\, J_o(\Delta R) - iK_o(MR)\, J_1(\Delta R)\right\} \end{aligned} \tag{IV.6}$$

and we can therefore fit experiments with a single phenomenological parameter R.

Values of R found in the fits varied between 0.7 and 1.3 fermis. As we see in Fig.10, which is a fit to the $p\bar{p} \to \Lambda\bar{\Lambda}$ data of Baltay et al (1962) the model is able to fit convincingly the diffraction peak away from the forward angles, but also predicts a diffraction minimum at small angles which does not appear in the experimental data. The same fault appeared in the diffraction ring model. Fits to most other processes, however, such as $K^+p(\pi)$ K*N* as shown in Fig. 11 do not suffer from this defect.

The anomalous diffraction minimum in the fit of $p\bar{p} \to \Lambda\bar{\Lambda}$ is a consequence of the sharp cut-off in the matrix elements and can be removed by rounding the edge of the distribution. To do this one must however introduce more parameters into the fit.

A more natural way of introducing absorption into the peripheral model is an extension of the distorted wave approximation of Sopkovich, and was first suggested by Durand and Chiu (1964a,b, 1965a,b) and Gottfried and Jackson [Gottfried and Jackson (1964c), Jackson (1965), Jackson et al (1965)] . This gives for the elements of the T matrix:

$$T_{fi}^{\ell} = e^{i\delta_f^{\ell}} B_{fi}^{\ell} e^{i\delta_i^{\ell}} , \qquad \text{(IV.7)}$$

where $\delta_i^{\ell}$ and $\delta_f^{\ell}$ are the initial and final complex scattering phase shifts, and $B_{fi}^{\ell}$ is the partial wave projection of the amplitude for unmodified single particle exchange. The success of this formula in fitting pseudoscalar exchange processes is indisputable, but, as we shall see, the theoretical justification is not so firmly based and the success is not maintained in

fitting processes with vector exchange. To understand the derivation of this formula we shall follow closely the potential theoretic derivation of Gottfried and Jackson (1964c) using the impact parameter representation. An alternative derivation of this result as the solution of two-channel coupled partial wave equations is given by Durand and Chiu (1965).

In the distorted wave Born approximation, the transition amplitude is approximated by the matrix element

$$T_{fi} = < \psi_f^{(-)} \left| V \right| \psi_i^{(+)} > , \qquad \text{(IV.8)}$$

where the interaction potential V causing the transition is considered weak enough to be treated as a perturbation. $\psi_i^{(+)}$ is the wave function of the system in the initial state. It represents an incoming wave for a particle propogating through a complex potential $U^{(+)}$. $\psi_f^{(-)}$, the analogous wave function in the final state represents an outgoing wave emerging from a potential $U^{(-)}$. We work to all orders in $U^{(\pm)}$, the optical potentials for the incoming and outgoing states respectively, and to first order in the perturbation V.

As we are working at high energies and with small momentum transfers, it is appropriate to use the Glauber (1958) approximation for the wave functions. This gives for $\psi^{(\pm)}$:

$$\psi_{q_\pm}^{(\pm)}(\underset{\sim}{b},z) \simeq \exp\left[i q_\pm \cdot \underset{\sim}{x}\right] \exp\left[(-i/v_\pm) \int_{\mp\infty}^{z} U^{(\pm)}(\underset{\sim}{b} + \hat{\underset{\sim}{\kappa}} z')\, dz'\right] \qquad \text{(IV.9)}$$

where $v_\pm$ is the relative velocity of the particles in the given state, $\underset{\sim}{q}_+$ and $\underset{\sim}{q}_-$ are the initial and final 3-momenta respectively, and we have assumed one 3-dimensional degree of freedom z chosen along $\underset{\sim}{\kappa} = \underset{\sim}{q}_+ + \underset{\sim}{q}_-$. The impact parameter vector $\underset{\sim}{b}$ is perpendicular to $\underset{\sim}{\kappa}$ and $\underset{\sim}{r} = \underset{\sim}{b} + \underset{\sim}{\kappa} z$. In this approximation, the expression for the scattering amplitude is:

$$T_{fi} \simeq \int d^2b \int_{-\infty}^{\infty} dz \exp\left[i \underset{\sim}{\Delta} \cdot \underset{\sim}{b}\right] V(\underset{\sim}{b} + \hat{\underset{\sim}{\kappa}} z) \times$$
$$\exp\left\{\frac{-i}{v_-} \int_z^{\infty} U^{(-)}(\underset{\sim}{b} + \hat{\underset{\sim}{\kappa}} z')^* \, dz'\right\} \exp\left\{\frac{-i}{v_+} \int_{-\infty}^{z} U^{+}(\underset{\sim}{b} + \hat{\underset{\sim}{\kappa}} z'') \, dz''\right\} \qquad \text{(IV.10)}$$

In order to make the equations more tractable, it is necessary to make further assumptions about $U^{(\pm)}$. The simplest is to assume that the elastic interactions are the same in the initial and final channels, i.e. $U^{(+)} = U^{(-)} = U$ and $v_+ = v_- \equiv v$. Equation (IV.10) then becomes

$$T_{fi} = 2\pi \int_0^{\infty} J_o(\Delta b) \exp\left[2i\delta(b)\right] B(b) \, b \, db \, , \qquad \text{(IV.11)}$$

where

$$2\delta(b) = -\frac{1}{v} \int_{-\infty}^{\infty} U(\underset{\sim}{b} + \underset{\sim}{\kappa} z) \, dz \qquad \text{(IV.12)}$$

is the phase shift of a wave packet traveling through the potential U, at an impact parameter $\underset{\sim}{b}$, and

$$B(b) = \int_{-\infty}^{\infty} V(\underset{\sim}{b} + \underset{\sim}{\kappa} z) \, dz \qquad \text{(IV.13)}$$

is the unmodified Born approximation for the amplitude. Another case in which a simple approximation can be found for $T_{fi}$ is when the range of V is much smaller than that of $U^{(+)}$ or $U^{(-)}$. In this case, Eq. (IV.10) reduces to:

$$T_{fi} = 2\pi \int_0^\infty b\, db\, J_0(\Delta b)\, B(b)\, \exp\left\{i\left[\delta^{(+)}(b) + \delta^{(-)}(b)\right]\right\} \quad . \tag{IV.14}$$

For the problems we are considering, however, this is hardly a valid assumption, and so the Gottfried-Jackson derivation is based on the assumption that the initial and final elastic scattering amplitudes are equal. A comparison of Eq. (IV.11) with Eq. (IV.3) now gives for the distorted wave Born approximation

$$T(b) = e^{2i\delta(b)}\, B(b) \quad , \tag{IV.15}$$

where we have set $\delta^{(+)} = \delta^{(-)} = \delta$. We now see that the model of Bugg and Dar and Tobocman comes directly from this equation by writing:

$$e^{i\delta(b)} = \begin{cases} 0 \text{ for } b < R \\ 1 \text{ for } b > R \end{cases} \tag{IV.16}$$

In order to calculate Eq. (IV.15) in any given case, a further approximation is also made for the scattering phase shift $\delta(b)$. If we assume that at high energies the elastic scattering cross-sections are

essentially imaginary, and that the experimental angular distributions are well fitted by a Gaussian form:

$$T_{elastic} = i \frac{\sigma_T q}{4\pi} \exp\left[-\frac{1}{2} A\Delta^2\right], \tag{IV.17}$$

with $\sigma_T$ the total cross-section, q the center-of-mass momentum and A a slowly varying function of energy, then we have for $\delta$:

$$\exp\left[2i\,\delta(b)\right] = 1 - C \exp\left[-b^2/2A\right], \tag{IV.18}$$

with $C = \sigma_T/4\pi A$. Note that $C \leq 1$, since, for imaginary $\delta$,

$$\exp\left[2i\,\delta(b)\right] \geq 0 \tag{IV.19}$$

Recent measurements [for example, Foley et al(1965)] have shown, however, an appreciable real part (up to 30 per cent) in $\pi p$ and pp cross-sections even at forward angles, indicating that the above parametrization is at best approximate. In actual calculations, Gottfried and Jackson have also generalized Eq. (IV.15) to the impact parameter form of Eq. (IV.7):

$$\begin{aligned} T(b) &= e^{i\delta_+(b)}\, B(b)\, e^{i\delta_-(b)} \\ &= \left[1 - C_+ e^{-\gamma_+(x-x_{min})^2}\right]^{1/2} B(b) \left[1 - C_- e^{-\gamma_-(x-x_{min})^2}\right]^{1/2} \end{aligned} \tag{IV.20}$$

where $C_+$ and $C_-$ are the amounts by which the lowest partial waves are absorbed in the initial and final states respectively, $2\gamma_\pm A_\pm q_\pm^2 = 1$ and $x = qb$; $x_{min}$ is introduced here so that it is possible to achieve full absorption in the S-wave with $C = 1$.

The inclusion of spin in the formalism necessary to predict the correct form of angular distributions and resonance decay correlations requires only a straightforward generalization of Eq. (IV.7) using the helicity formalism of Jacob and Wick (1959), and one writes:

$$< \lambda'\mu' \left| T^\ell \right| \lambda\mu > = e^{i\delta_f^\ell} < \lambda'\mu' \left| B^\ell \right| \lambda\mu > e^{i\delta_i^\ell} \qquad \text{(IV.21)}$$

where $\lambda\mu$, $\lambda'\mu'$ are the helicities of initial and final particle states respectively. In generalizing the spinless equation to this form we have made the additional assumption that the diffraction scattering in the "blobs" of Fig. 8 does not change the initial or final state helicities.

B. Decay Correlations

In our discussion of the mechanisms responsible for the production of resonant states, we have so far treated the resonances as stable particles. In any experiment, however, one usually recognizes these resonances by studying their decay products, and, as we discussed in Section II, the angular distribution of these decay products contains information on the method of formation of the particle which is additional to that obtained from momentum and energy distributions. We shall consider again the

reaction $\pi p(\pi)\rho p$, but our remarks are readily generalized to other processes, and a discussion of the general case may be found in Gottfried and Jackson (1964b).

We begin by writing the amplitude for the decay $\rho \rightarrow \pi\pi$ in the rest frame of the $\rho$. It is possible to show, using general helicity arguments, that this has the form

$$A_m(\theta,\varphi) = (3/4\pi)^{1/2}\, d^1_{mo}(\theta)\, \exp\left[i\varphi m\right], \tag{IV.22}$$

where $d^1_{mo}(\theta)$ is a reduced rotation matrix [Jacob and Wick (1959)] and where we have expressed our polar angles $\theta,\varphi$ with respect to $\underline{p}$, the momentum of one of the decay pions as shown in Fig. 6; m is the component of the $\rho$'s spin in an arbitrary direction of quantization.

The probability for decay in the direction $(\theta,\varphi)$ of the produced $\rho$ may now be written as a function of A in the form

$$W(\theta,\varphi) = \sum_{m,m'} A_m\, A^*_{m'}\, \rho_{mm'} \tag{IV.23}$$

where $\rho_{mm'}$ is the canonical spin-space density matrix of the $\rho$. Choosing again the 3-momentum axis of the incident pion as the spin quantization direction we may express $\rho_{mm'}$ in terms of the helicity matrix elements $< \mu'\lambda' \left| T \right| \lambda >$ of the process $\pi p_\lambda \rightarrow \rho_{\mu'}\, p_{\lambda'}$

$$\rho_{mm'} = N \sum_{\mu\mu'\lambda\lambda'} d^1_{m\mu}(\Psi) < \mu\lambda' \left| T \right| \lambda >^* < \mu'\lambda' \left| T \right| \lambda > d^1_{m'\mu'}(-\Psi) \tag{IV.24}$$

In this equation, the angle $\Psi$ is defined by

$$\sin \Psi = 2m_\rho p \sin \theta \left\{ \left[ t - (m_\rho + \mu)^2 \right] \left[ t - (m_\rho - \mu)^2 \right] \right\}^{1/2} ,$$

N is chosen to give $\rho_{mm'}$, a unit trace, and $m_\rho$ is the mass of the $\rho$. In terms of Eqs. (IV.22) and (IV.23) we can now write for $W(\theta,\varphi)$:

$$W(\theta,\varphi) = (3/4\pi) \sum_{m,m'} \exp \left[ i(m-m')\varphi \right] d^1_{mo}(\theta)\, d^1_{m',o}(\theta)\, \rho_{mm'} , \qquad \text{(IV.25)}$$

which gives the complete angular dependence of the decay cross-section directly in terms of the density matrix elements, or alternatively, in terms of the matrix elements of the production reaction.

In addition to the trace condition, we may further relate the elements of the density matrix by the Hermiticity condition

$$\rho_{mm'} = (\rho_{mm'})^+ , \qquad \text{(IV.26)}$$

and by parity conservation, which requires that

$$\rho_{-m,-m'} = (-1)^{m-m'} \rho_{mm'} \qquad \text{(IV.27)}$$

Thus for a resonance with J = 1, the density matrix has the explicit form

$$\rho_{mm'} = \begin{pmatrix} \rho_{11} & \rho_{10} & \rho_{1,-1} \\ \rho^*_{10} & \rho_{00} & -\rho^*_{10} \\ \rho_{1,-1} & -\rho_{10} & \rho_{11} \end{pmatrix} \qquad \text{(IV.28)}$$

where all elements are real except $\rho_{10}$, and

$$\rho_{oo} = 1 - 2\rho_{11} \tag{IV.29}$$

In terms of these elements, the explicit form of the $\rho$ decay distribution is then

$$W(\theta,\varphi) = (3/4\pi) \left\{ \rho_{oo} \cos^2\theta + \rho_{11} \sin^2\theta - \rho_{1,-1} \sin^2\theta \cos 2\varphi - \sqrt{2}\, \mathrm{Re}\, \rho_{10} \sin 2\theta \cos\varphi \right\} , \tag{IV.30}$$

where we see that all the density matrix elements except Im $\rho_{10}$ are known from a measurement of the decay distribution.

Our discussions earlier show us that for unmodified pion exchange, with or without form factor corrections, only $\rho_{oo}$ is non-zero (and unity in this case), but this is no longer true if appreciable absorption corrections or contributions from other particle exchanges occur. Of course, such allowed exchanges in this case are limited, the next lightest exchange being an $\omega$ which contributes only to $\rho_{11}$ and $\rho_{1,-1}$. Present data [for example, Hagopian et al (1965)] indicates significant contributions from both $\rho_{10}$ and $\rho_{1,-1}$ (Fig. 12). The existence of a non-zero $\rho_{10}$ term in particular is strong evidence against any form factor model of this process which allows only one pion and $\omega$ exchange without initial and final state absorption.

C. Applications

The absorption model has been applied now to a large variety of processes mediated by pseudoscalar and vector exchange. These include

$\pi N \rightarrow \rho N$ [Durand and Chiu (1965a), Gottfried and Jackson (1964c), Hagopian et al (1965), Jackson et al (1965)] ,

$\pi p \rightarrow \rho N^*(1238)$ [ABBBHLM Collaboration (1965), Jackson et al (1965)] ,

$\pi p \rightarrow \omega N^*(1238)$ [ABBBHLM Collaboration (1965), Svensson (1965a)] ,

$\pi^- p \rightarrow \pi^0 n$ [Barger and Ebel (1965), Högaasen and Högaasen (1965)] ,

$\pi^+ n \rightarrow \omega p$ [Jackson et al (1965)] ,

$\pi N \rightarrow N +$ spin $2^+$ [Högaasen et al (1965)] ,

$Kp \rightarrow KN^*$, $Kp \rightarrow K^*N^*$, $Kp \rightarrow K^*N$, $Kp \rightarrow \pi Y^*$, and the analogous reactions with $\bar{K}$ [Jackson et al (1965)] ,

$pp \rightarrow nN^*$ [Alexander et al (1965)] ,

$np \rightarrow pn$ (charge exchange) [Durand and Chiu (1965a), Ringland and Phillips (1964)] ,

$N\bar{N} \rightarrow Y\bar{Y}$ [Durand and Chiu (1965a), Högaasen and Högaasen (1965)] ,

$N\bar{N} \rightarrow N^*\bar{N}^*$ [Svensson (1965b)] .

The common feature of many of these interactions is the dominance of the forward peak, and in most cases the distributions are confined almost entirely to momentum transfers less than $0.5(\text{GeV}/c)^2$. In the most pronounced case, $\pi p \rightarrow \rho p$, the important range of momentum transfers has an average of approximately $0.15\ (\text{GeV}/c)^2$.

Cross-sections have also been calculated using a modified OPE model for several processes involving photoproduction of resonant states [Cambridge Bubble Chamber Group (1965), Locher and Sandhas (1965)] . In these cases,

one assumes of course that absorption occurs only in the strongly interacting final state as shown in Fig. 13.

A detailed discussion of all these reactions is given in the cited references and we shall therefore restrict ourselves to discussing the fits to a few processes which show general trends of the model.

We begin by considering the process $\pi p \rightarrow \rho p$ which we have assumed previously is mediated by a one-pion-exchange mechanism. This interpretation is confirmed by a study of the $\rho$ decay distribution which is essentially of the form $\cos^2\theta$. We show in Fig. 14 a comparison of the absorption model fit to $\pi^+ p \rightarrow \rho^+ p$ at 2.75 GeV/c with the Amaldi-Selleri form factor fit discussed in the last Section. Included in the figure is the unmodified OPE cross-section for the reaction, which has the form

$$\frac{d\sigma}{dt} = \frac{\pi}{4m_\rho^2 M^2 p_{inc}^2} \frac{g^2}{4\pi} \frac{g_\rho^2}{4\pi} \frac{t\left[t - (m_\rho + \mu)^2\right]\left[t - (m_\rho - \mu)^2\right]}{(t - \mu^2)^2} \qquad \text{(IV.31)}$$

where $p_{inc}$ is the incident momentum of the pion in the laboratory system, and $g$, $g_\rho$ are the $\pi NN$ and $\rho\pi\pi$ rationalized, renormalized, coupling constants respectively. The assumption of "complete absorption" is made in this and all subsequent fits using the absorption model. We see that the unmodified OPE cross-section is too large by a factor of 50 per cent at the low momentum peak and predicts too slow a fall-off with increasing momentum transfer. On the other hand, as the absorption model cannot be preferred to the form factor fit to the cross-section, it is necessary to make a detailed examination of the $\rho$ spin density matrix in order to

distinguish between them. The form factor fits predict $\rho_{00} = 1$ and all other elements zero, while the absorption model predicts $\rho_{00} \sim 0.7$ with small contributions to the other elements. Presently available data (Fig. 12) is consistent with the latter value.

Fits have been made to the various modes of $\pi N \rightarrow \rho N$ up to 8 GeV/c, and in all cases, provided one assumes complete absorption, an effective fit can be made. Variations necessary in the initial state absorption factors are consistent with one's knowledge of the elastic scattering. In particular, the energy dependence of the total cross-section is well fitted by the theory as shown in Fig. 15. We note, however, that the variation with energy is already correctly given by unmodified one-pion-exchange. On integrating Eq. (IV.31) with respect to t, and ignoring the almost negligible t dependence of the lower limit of integration at the energies we are considering, we see that the total cross-section has the form:

$$\sigma = c/q_{inc}^2 , \qquad \text{(IV.32)}$$

where c is an energy independent constant. This qualitative prediction of $1/q_{inc}^2$ dependence in the cross-section agrees well with experiment. As the addition of any t dependent variations in the model can only change the normalization of the cross-section, any correctly normalized theory based on one-pion-exchange must automatically predict the correct energy dependence of the total cross-section. It is not surprising therefore that the absorption model can fit the energy distributions, as the only energy dependence in its modification of one-pion-exchange comes from the elastic total cross-section $\sigma_T$ and the width of the

diffraction peak in Eq. (IV.17) both of which have a small variation with energy. When the "complete absorption" philosophy is applied, this dependence is not sufficient to produce appreciable deviations in the general energy behavior of the inelastic cross-section. On the other hand, there appears to be a small but systematic difference between the cross-sections for $\pi^+ p \to \rho^+ p$ and $\pi^- p \to \rho^- p$ which grows with energy and which the model in its present form cannot explain. This may perhaps be due to the neglect of the real parts of the elastic amplitudes in the model which appear to be quite different in magnitude for the two charged elastic modes [Foley et al (1965)].

A study of the decay distributions in many other processes also indicates a single pion exchange mechanism, but with sufficient variation from the unmodified model predictions to require either a mechanism like absorption or corrections from higher mass or spin exchange. For example, the process $K^+ p \to K^* N^*$ is particularly interesting because one can study the decay distribution of both the $K^*$ and $N^*$, and in each case one sees strong evidence for one-pion-exchange. The deviations in the density matrix elements from one-pion-exchange in each case can be fitted by absorption corrections and do not seem to indicate a need for higher spin exchange. Data for this process is only available at present in the 2-3 BeV/c region, so no test can be made here of the energy dependence of the theory.

The cases we have considered so far provide the easiest test of the various models in fitting the data, as they involve both spin zero exchange and a pole very near the physical region. In order to test the

validity of the fits to spin zero exchange processes in general, it would be useful to examine reactions dominated by the exchange of a single spin zero particle of heavier mass, for example, a K meson. Unfortunately, relatively little data is available on such reactions, so we must turn our attention to the fits which have been made to processes which also involve vector exchange. Several reactions have been observed whose decay distributions indicate evidence for both spin zero and spin 1 exchange. For example, we show in Fig. 16 the angular distributions at 3 GeV/c for the decay products ($K^o$ and $\pi^+$) from the resonance K* produced in the reaction $K^+p \rightarrow K^*p$. The density matrix elements are also shown in Fig. 17. The marked cos $2\theta$ dependence in the decay distributions suggests a dominant vector exchange contribution, and this is confirmed by a detailed study of the density matrix elements. We notice that for cos $\theta < 0.9$ only $\rho_{1,1}$ and $\rho_{1,-1}$ are appreciably different from zero, and that the only evidence for one-pion-exchange is seen at very forward angles.

Successful fits to the process at this energy have been made using the complete absorption model, assuming both $\pi$ and $\rho$ exchange as shown in Fig. 18. A fit was also made to data at 5 GeV/c using the same coupling constants (Fig. 19), but it was found that although the agreement was satisfactory for $\Delta^2 \lesssim 15\ \mu^2$, the theoretical estimate was much too high at larger momentum transfers. The failure of the fit to the energy dependence of the data was indicated by the theoretical total cross-section estimate of 0.85 mb compared with the experimental value of 0.3 mb. The lack of success of this model in fitting energy distributions is even more marked when one considers a processes where only vector exchange is allowed

such as $\pi^- p(\rho)\ \pi^0 n$ and $\pi^+ n(\rho)\ \omega p$. In these cases the model is off by orders of magnitude in fitting the high energy distributions. This failure again reflects the fact that the "complete absorption" model is essentially a scheme for t modification of the one-particle exchange amplitude. The cross-section as calculated from unmodified $\rho$ exchange gives a distribution which remains constant with energy, and so the absorption model has little hope of predicting the fall-off of the cross-section with increasing energy which is found in the data. A more detailed discussion of this point may be found in Högaasen and Högaasen (1965a). To improve such fits requires further drastic assumptions which we shall discuss in the next Section.

## V. K-MATRIX MODELS OF PERIPHERAL PROCESSES

In spite of the relative success of the absorption model in fitting processes involving pseudoscalar exchange, it is obvious that the procedure still involves a certain amount of curve fitting. Although the initial state absorption parameters are given to us by experiment, the "complete absorption" philosophy used to determine the final state parameters is apparently an ad hoc prescription which seems to work. However, the fits to processes involving vector exchange are as unsatisfactory as ever; the energy variation predicted being in gross disagreement with experiment.

The model we discussed in the last Section in the form given by Eq. (IV.7) is not the only way of introducing the apparently necessary damping of the low partial waves in the one particle exchange matrix elements, however, and in this Section, we shall consider other approaches which have been used recently to fit peripheral processes. We shall see that none of the methods appear to fit the energy behavior of vector exchange processes satisfactorily, but at least we can gain a better idea of why they fail.

In order to understand the derivation of these models we must restrict ourselves to two-particle reactions, allowing, of course, a final state resonance to be treated as a single particle. As most of the reactions we have discussed so far fall into this category, this is not too serious a restriction.

A natural framework for describing such reactions is provided by the N/D equations first introduced by Chew and Mandelstam (1960, 1961) in their study of the pion-pion interaction. If we wish to relate a series of two-body reactions using this formalism, we may write, in matrix form

$$\underset{\sim}{T}^{\ell} = \underset{\sim}{N}^{\ell} \; \underset{\sim}{D}^{\ell\,-1} \tag{V.1}$$

where we define a particular partial wave amplitude $T_{ij}^{\ell}(s)$ in terms of the S-matrix by

$$T_{ij}^{\ell}(s) = \left(S_{ij}^{\ell}(s) - \delta_{ij}\right) / 2i\rho_i\rho_j \tag{V.2}$$

In this equation,

$$\rho_i = (2k_i/W)^{1/2} \tag{V.3}$$

is a phase space factor associated with the $i^{th}$ channel, and $k_i$, W are the center-of-mass three-momentum and energy in that channel.

In Eq. (V.1), D is a real analytic function of energy except for a right-hand cut on the real axis from the first two-particle threshold to infinity. N, similarly, is a real analytic function except for poles and a left-hand cut.

In order to have a simple form for the unitarity equation it is necessary to make the further drastic approximation of retaining only

two-particle intermediate states. The unitarity condition can then be expressed for each partial wave in the form

$$\mathrm{Im}\underset{\sim}{T}^{\ell} = \underset{\sim}{T}^{\ell}\,\underset{\sim}{P}\underset{\sim}{T}^{\ell} \tag{V.4}$$

where the operator P has elements

$$P_{ij} = \delta_{ij}\,\theta(s - s_i)\,\rho_i\rho_j \tag{V.5}$$

We thus have that

$$\mathrm{Im}\underset{\sim}{D}^{\ell} = -\,\underset{\sim}{P}\underset{\sim}{N}^{\ell} \tag{V.6}$$

Knowing the analytic properties of D and its imaginary part we may therefore write a dispersion relation in the form

$$\underset{\sim}{D} = I - \frac{s - s_o}{\pi}\int_{s_o}^{\infty}\frac{ds'\,PN(s')}{(s' - s)(s' - s_o)} \tag{V.7}$$

In writing Eq. (V.7) we have made one subtraction and normalized D at $s_o$ to unity. Writing now

$$\underset{\sim}{D} = \mathrm{Re}\underset{\sim}{D} - i\underset{\sim}{P}\underset{\sim}{N} \tag{V.8}$$

we see that Eq. (V.1) may be written in the form

$$\underset{\sim}{T} = \underset{\sim}{N}/(\mathrm{Re}\underset{\sim}{D} - i\underset{\sim}{P}\underset{\sim}{N}) \tag{V.9}$$

or

$$\underline{T} = \underline{K}/(\underline{I} - i\underline{\rho}\underline{K}) \tag{V.10}$$

where

$$\underline{K} = \underline{N}/\mathrm{Re}\underline{D} \tag{V.11}$$

Equation (V.10) is the (multichannel) K-matrix equation [Heitler (1944), Dalitz (1961), Goldberger and Watson (1964)] and it has formed the basis for several models designed to fit peripheral processes. In order to use these equations in any actual calculation, it is necessary to make further simplifying assumptions about the form of N and Re D. The singularities of N provide the exchange forces which drive the interaction, and the strongest contributions to these come from the longest-range forces, or the cross-channel poles nearest the physical region. If we also assume that the principal value integral in D may be neglected, we can write for K,

$$K^{\ell} = B^{\ell} \tag{V.12}$$

where $B^{\ell}$ is the contribution from the one-particle exchange terms in the $\ell^{th}$ partial wave. Most calculations using the K-matrix equations employ this approximation for the inelastic elements, although the early calculations of Baker and Blankenbecler (1962) which used the impact parameter

form of Eq. (V.10) developed by Blankenbecler and Goldberger (1962) also considered other models for K. We shall discuss the fits made using the K-matrix approach later in this Section. A calculation of Ross and Shaw (1964), which considered the effect of absorption on the apparent position and width of the $\rho$ in $\pi N \rightarrow \rho N$ was also equivalent in predictions to the model of Baker and Blankenbecler, although it does not have a well defined K-matrix structure.

The significance of the approximations Eqs. (V.10) and (V.12) is easiest illustrated by a diagrammatic representation of the one-channel K-matrix equations as shown in Fig. 20. If intermediate state particles a' and b' are on the mass-shell, which is equivalent to setting Re D = 1 in Eq. (V.11), then Fig. 20a represents the one channel equation

$$T = B + iBT \tag{V.13}$$

which may be further expanded as shown in Fig. 20b as a series of ladder graphs.

In order to fit an elastic scattering process such as $\pi p \rightarrow \rho p$, however, it is evident that the coupling of at least the two channels $\pi p$ and $\rho p$ must be considered in order to fit the data. It is found, however, that a simple two-channel model is a very poor fit to the data and the reason is not hard to see. Even at energies of the order of 2GeV we say in Section IV that the $\pi p$ and $\rho p$ channels represent only a fraction of the total cross-section for $\pi p$ scattering and the coupling of the other channels to the $\pi p$ channel will have a marked effect on the

process under consideration. This fact was, of course, one of the main reasons for introducing the idea of absorption in the first place. In addition, it is not clear that Eq. (V.12) is a valid approximation in the elastic channels which presumably are all strongly absorptive. Nevertheless, to improve the calculation at least requires contributions from more channels. However, even if we restrict ourselves to two-particle channels which couple to the $\pi p$ system, there are a bewildering number to be considered, e.g. $\pi N^*$ (1238), $\rho N^*$, $\omega N^*$, $\omega p$, $\pi N^*$ (1512), etc. To include all these in a calculation, assuming that the K-matrix elements are approximated by Born terms, requires a knowledge of all coupling constants involved in the relevant Born amplitude. Most of these are still unknown, so, even at this level, such a calculation becomes necessarily phenomenological; all one can do is show that experiments can be fitted with reasonable values for the many coupling constants involved using, for example, a symmetry scheme such as SU(6) as a guide in determining the relative magnitude of the coupling.

In addition if one wishes to extend the formalism further to include three or more particle channels then the simple form of the unitarity equation, Eq. (V.6) is replaced by a complicated integral equation, and the simplicity of Eq. (V.10) is lost.

On the other hand, it is possible that all but the most important channels each have a small effect on the process considered and moreover are produced in a reasonably incoherent manner, so that their total effect may be estimated by appeal to some form of randomness hypothesis. This idea has been taken furthest by Squires [1964, 1965 a,b, Kumar and

Squires (1965)] and Trefil (1966), although all K-matrix fits make some effort to include the effect of neglected channels.

The basic assumption in this approximation is that the many unknown coupled channels contribute to the scattering with equal weight but random signs. The simplest approximation is to assume that <u>all</u> elements of the K-matrix have the same order of magnitude, but random signs. The random phase hypothesis then requires that the off-diagonal elements of $K^2$ be small compared with the diagonal elements, and it is possible to show by standard statistical arguments [Squires (1965a) Wigner (1955)] that

$$T_{12} = \frac{(1 + e^{-2\gamma})^2}{4} B_{12} \qquad (V.14)$$

where $B_{12}$ as before is the inelastic one particle exchange amplitude and $\gamma$ is the imaginary part of the elastic phase shift.

Of course it is physically unreasonable that all elements of K have the same magnitude, and several improvements of this basic idea have been suggested. These assume either that all the unknown terms of the K-matrix - that is, those we cannot calculate - have the same weight and random phase, but this weight is different from that of the known (calculable) part, or that the unknown channels which couple directly to those under consideration have a greater weight than the remaining unknown terms coupling with each other. Each of these approximations naturally introduce further arbitrary parameters into the theory.

Fits to a variety of processes using the K-matrix model have now been made. Dietz and Pilkuhn (1965a,b) made an exhaustive study of

$K^+p \to K^{*+}p$, including explicitly the effects of the $K^+p$, $K\Delta^*$, $K^*N$ and $K^*\Delta^*$ channels and allowing for three and multiparticle channels with a simple random phase hypothesis. Although satisfactory fits to the inelastic process were obtained they required an excessively large contribution from three body channels in the low partial waves, which in fact almost masked the S-wave completely. Arnold (1964) considered fits to several processes with reasonable success, although no attempt was made to test the energy dependence to the theory. His fit to $\bar{K}N$ charge exchange at 1.80 GeV/c is shown in Fig. 21. Finally Trefil (1966) carried out a detailed study of forward and backward charge exchange pion-nucleon scattering, and found that although the data at a given energy can be fitted, the energy dependence of the theory is in disagreement with experiment with the two random phase models used to include unknown channels. Thus the K-matrix model in the form we have discussed fails to explain the energy dependence of processes dominated by vector exchange, and requires a stronger damping of the low partial waves than seems given by the theory, just as we found in the absorption model.

The reasons for the similarity in the failure of the two approaches would be more understandable if it were possible to derive the absorption model using an approach based on the N/D equations or dispersion theory rather than potential theory. This has been attempted by several authors [Ball and Frazer (1965), Griffiths and Saperstein (1965), Omnes (1964), Watson (1965)], but requires very stringent restrictions on the form of the scattering amplitudes involved. The only reliable conclusion to be drawn is that the K-matrix and absorption models are consistent when the absorption

is weak, but no convincing proof can be found in the more important case of strong absorption. In particular, a two channel model of a scattering process is clearly inconsistent with the absorption model in the limit of strong absorption. The explicit expression for the inelastic amplitude in a unitarized two channel model is

$$T_{12}^{\ell} = e^{i\delta_1^{\ell}} \sqrt{\left[\frac{1}{\eta_\ell^2} - 1\right]}\, e^{i\delta_2^{\ell}} /2\rho_1\rho_2 \qquad (V.15)$$

where $\delta_1$ and $\delta_2$ are the initial and final complex scattering phase shifts respectively, and

$$\eta_\ell = \left|e^{2i\delta_1^{\ell}}\right| = \left|e^{2i\delta_2^{\ell}}\right| \qquad (V.16)$$

is the absorption coefficient.

A comparison with Eq. (IV.7) shows then that the absorption model in this case associates the unmodified amplitude with the term $\sqrt{\left[\frac{1}{\eta_\ell^2} - 1\right]}\, /2\rho_1\rho_2$ and this is clearly impossible in the strong absorption limit ($\eta \to 0$). We note also that in terms of the elements of the two channel K-matrix, $T_{12}$ has the form

$$\begin{aligned} T_{12}^{\ell} &= K_{12}^{\ell}/\Delta_\ell \\ &= e^{i\delta_1^{\ell}}\, K_{12}^{\ell}\, e^{i\delta_2^{\ell}}/\eta_\ell \left|\Delta_\ell\right| \end{aligned} \qquad (V.17)$$

where

$$\Delta_\ell = (1 - i\rho_1 K_{11}^{\ell})(1 - i\rho_2 K_{22}^{\ell}) + \rho_1\rho_2 (K_{12}^{\ell})^2 \qquad (V.18)$$

If one now approximates $K_{12}$ by $B_{12}$, we have equivalence with the absorption model only in the limit of weak absorption ($\eta \to 1$) and high energies ($\Delta \to 1$). This is not, of course, an argument against the absorption model, which is designed to apply in the case of many channels rather than few, but merely points out the inadequacy of trying to study the problem at a two channel level.

The more easily understandable structure of the K-matrix model, however, allows us to investigate further the reasons for its failure in the cases we have discussed. Presumably similar reasons also apply in the case of the absorption model. Apart from the restriction to two body processes, which can be relaxed if one is prepared to solve unitarity equations, the most drastic assumption made in deriving the model is that K can be approximated by the Born term, or in other words, that the cuts in N and D can be neglected. Probably a more realistic assumption to make is that the off-mass-shell behavior of the exchanged particle is important, as we assumed in the form factor model, and so approximate K by a Born term with form factors. Presumably one can use much less drastic form factors in this case than were needed by Ferrari and Selleri (1963), as unitarity is automatically built into our equations. Calculations by Bander and Shaw (1965) using the absorption model of $\pi N \to \rho N$ also indicate that these corrections must be small otherwise the effect of absorption corrections on the density matrix of the $\rho$ is reduced and the decay correlation data can no longer be fitted. However, as we discussed in the last Section, such t dependent form factor

corrections have no effect on the energy dependence of the theory; this can only come from a mechanism which changes the energy dependence of the K-matrix. As the momentum transfer collimation of this theory that is, a suppression of high momentum transfer events, comes from the summation of the set of ladder diagrams in the scattering channel as shown in Fig. 20, it is reasonable to assume that a reduction to the high energy behavior will come similarly from a sum of ladder iterations of the K-matrix element in the crossed (t) channel as shown in Fig. 22. It was shown by Amati et al (1962) that the summation of such graphical series leads naturally to a Regge pole behavior for the elastic scattering amplitudes. The inclusion of "Reggeized" K-matrix elements in the vector exchange model would cause a collimation of the energy distributions required by the data. It is not clear however [Arnold (1965), Jackson (1965), Barger and Ebel (1965)] whether a similar application of the absorption model to a Reggeized vector exchange is consistent, as the absorption model may already contain corrections of the form shown in Fig. 22. Presumably, though, a correction of this sort must be necessary if the model is to have the correct energy dependence for vector exchange. On the other hand, a calculation in a K-matrix framework avoids this possible ambiguity.

Of course, we have suggested the impossible; a calculation involving form factors, Regge poles and corrections for unknown channels would involve so many arbitrary parameters as to be almost meaningless. Still, it is apparent from our discussion that all effects may be there, and it may be indeed true that strong interactions are too rich in detail to allow accurate quantitative analysis over a complete spectrum of energies and momentum transfers.

On the other hand, given an understanding of the mechanisms involved we have seen that we can still draw qualitative conclusions from processes which are peripheral in nature and this allows us for example to make order of magnitude predictions of the size of particle beams at higher energies, as we discuss in the next Section.

## VI. BEAMS

In this concluding Section we revert to a much more primitive level of theoretical discussion in order to consider the photoproduction of secondary beams of strongly interacting particles. (Drell, 1965) Up to this point we have looked at transition amplitudes for two strongly interacting particles (stable or unstable) in the initial and final states and analyzed the quantitative successes and shortcomings of the theoretical analyses in fitting magnitudes of cross-sections, their energy and momentum transfer dependence, and the observed decay correlations. The applications to photoproduction processes which we now discuss make much less stringent demands on the theory since we are concerned only with approximate predictions of fluxes of high energy pions, K mesons, and anti-baryons which can then serve as projectiles in subsequent experiments. We are more interested here in the practical use to which these beams can be put than in casting light upon the detailed theoretical nature of the interactions involved.

We consider first charged pion beam production via one pion exchange as illustrated in Fig. 23. Under kinematical conditions such that a high energy photon of momentum k produces a high energy pion with energy $\omega_q \sim k \gg \mu$, at a small angle $\theta_q \sim \mu/k$, then the impact parameter is large, ($\sim 1/\mu = 1.4$ fermis) and an almost real pion is exchanged between vertices (A) and (B) in Fig. 23. The corresponding contribution (Drell, 1960) to the differential cross-section in this very restricted

phase space interval is, in the peripheral approximation,

$$d^2\sigma_{\gamma,\pi^\pm}(k,\omega_q,\theta_q) = \frac{\alpha}{2\pi}\frac{\sin^2\theta_q}{(1-\beta_q\cos\theta_q)^2}\frac{d\Omega_q}{4\pi}\frac{\omega_q(k-\omega_q)\,d\omega_q}{k^3} \times \sigma^{tot}_{\pi^\mp}(k-\omega_q) \qquad \text{(VI.1}$$

The numerator factor $\sin^2\theta_q$ comes from angular momentum conservation since a transversely polarized photon cannot transfer its spin to a pion moving forward. $\sigma^{tot}_{\pi^\mp}(k-\omega_q)$ is the total $\pi^\mp$ - proton cross-section at a laboratory energy $k-\omega_q$ and is an exact expression of the interaction vertex (B) if we extrapolate to the pion exchange pole at $(k-q)^2 \simeq \mu^2$, or $(1-\beta_q\cos\theta_q) \to 0$. The accuracy of this extrapolation is questionable for nuclear targets with atomic number $A > 1$ in which case the interval of extrapolation from the physical region to the pion exchange pole, ($\sim 2\mu = 300$ MeV), is large compared to the excitation energies of the target instead of being small as we require. (Bell, 1964) The accuracy of this approximation for hydrogen targets is however the basic assumption of the peripheral model.

Keeping this reservation in mind we show in Fig. 24 the experimental results for $\pi^-$ photoproduction from beryllium [Blanpied et al (1963), Blumenthal et al (1963)]. The agreement to within a factor of two near the peak of the theoretical distribution supports the optimism of the peripheral model in its predictions that intense charged pion beams may be produced by high energy electron accelerators. However, the difference between theory and experiment and in particular the

failure of the observed angular distribution to drop at the forward angle, $\mu/k > \theta_q \to 0$ suggests the importance of the inclusion of other diagrams in addition to the various corrections which have been made to the one-pion-exchange result, Eq. (VI.1), and which are discussed with references by Drell (1965).

A leading candidate to explain this difference is the amplitude for coherent diffraction production of $\rho^o$ mesons in the forward direction followed by their decay into a $\pi^+$, $\pi^-$ pair as shown in Fig. 25. A forward diffraction peak in high energy photoproduction of zero strangeness neutral vector mesons is theoretically expected since they have quantum numbers in common with the photon. This peak has also been observed [Crouch (1964), Lanzerotti (1965)] with a very large cross-section, viz

$$\left[\frac{d\sigma(k,0^o)}{d\Omega}\right]_{\gamma\rho_o} \simeq A^{1.7}\left[\frac{k^2}{20\ \text{GeV}^2}\right] \text{ mb/ster} \qquad \text{(VI.2)}$$

The magnitude of this cross-section in hydrogen is in agreement with the predictions of a simple model [Berman and Drell (1964)] and also with dimensional arguments, since

$$\left[\frac{d\sigma(k,0^o)}{d\Omega}\right]_{\gamma\rho_o} \sim \frac{1}{137}\left[\frac{d\sigma(k,0^o)}{d\Omega}\right]_{\pi}$$

where $\left[\frac{d\sigma(k,0^o)}{d\Omega}\right]_{\pi}$ denotes the forward peak of elastic pion-nucleon scattering. A discussion of the $A^{1.7}$ variation of this result may be found in Drell and Trefil (1966).

The resulting flux of $\pi^{\pm}$ from the $\rho^{o}$ decay is readily computed in terms of the observed parameters of the $\rho^{o}$ production cross-section. It peaks at an angle

$$\theta_{max} \simeq \frac{m_\rho}{k} \sqrt{\frac{k - \omega_-}{\omega_-}} \quad , \tag{VI.3}$$

where $m_\rho$ is the $\rho^{o}$ mass, k the incident photon energy and $\omega_-$ the energy of the pion detected at an angle $\theta$. In the neighborhood of this peak, the cross-section may be written, for $k - \omega_- < \omega_-$,

$$\frac{d^2\sigma}{d\omega_- d\Omega} \simeq \left[\left(\frac{d\sigma(k,0^o)}{d\Omega}\right)_{\gamma\rho_o}\right] \frac{3e^{-b\, m_\rho^2/4k^2}}{\sqrt{\pi b}} \cdot \frac{(\omega_-/k)^{3/2}\sqrt{1 - \omega_-/k}}{k} \times$$
$$\exp\left\{- b(k/m_\rho)^2 (\theta-\theta_{max})^2\right\} \tag{VI.4}$$

where $b \approx 6A^{2/3}$ is a dimensionless parameter fit to the observed width of the $\rho^{o}$ diffraction peak.

The resulting pion flux from diffraction production on beryllium targets is computed [N. Hicks (1965 unpublished)] to exceed that via the pion exchange, Eq. (VI.1), as shown in Fig. 26 when averaged over the experimental conditions. Since Eq. (VI.4) increases roughly in proportion to $A^{4/3}$ it is reduced relative to the one pion exchange result Eq. (VI.1) for hydrogen targets. At the peak angle $\theta_q = \mu/\omega_q$ the one-pion-exchange cross-section is proportional to k for fixed ratio of pion to photon energy, $\omega_q/k$. A similar energy dependence is predicted by Eq. (VI.4)

at the peak angle $\theta = \theta_{max}$ and at sufficiently high energies such that $b\, m_\rho^2/4k^2 \approx 1.5\, (m_\rho/k)^2\, A^{2/3} < 1$. Their variation with fraction of energy $(1 - \omega_q/k)$ transferred to the observed pion differs however and by a study of this dependence together with the angular and A variation it will be possible to clarify further the relative importance of these two mechanisms for beams.

If one is interested in the behavior of momentum distributions near the low momentum peak, then it is found that absorption factors of the type discussed in Section IV are quantitatively of minor importance for pion exchange and for large impact parameter collisions with $b \sim 1/\mu$. At 8 GeV, for example, the absorption calculation leads to no reduction in the magnitude of the peak in $\pi p \rightarrow \rho p$, in spite of the large collimation produced in the tail. In any case, photo-induced reactions have no initial state absorption factors to reduce the calculated cross-sections, and the relevance of absorption factors for multiparticle final states as in Fig. 23 is not theoretically established or observed [Jones (1965)]. No such absorption factors appear in the theoretical models of the diffraction production which calculate ratios to observed strong interaction diffraction processes. Therefore these pion beam predictions should be applicable at higher energies than shown in Fig. 24.

Turning to charged K-meson beams the pole for K-meson exchange is approximately $m_K \approx 500$ MeV distant from the physical region. Equation (VI.1) with the K-meson replacing that $\pi$-meson mass has been experimentally checked only very roughly so far but preliminary indications are similar to what was seen in pion production. [Blanpied et al (1965)]. Neutral

K beams, and in particular $K_2$ beams, of comparable intensity are expected from the $K^*$ exchange amplitude Fig. 27 as has been analyzed in detail and with full inclusion of final state absorption factors [Drell and Jacob (1965)].

Finally we make some predictions on the production of anti-nucleon or anti-baryon beams by comparison with the observation of backward peaks in pion-nucleon scattering by Orear et al (1965) and their analysis by Trefil (1966). The basic mechanism in the calculation of

$$\gamma + p \rightarrow \bar{p} + (\text{anything})$$

as in

$$\pi + p \rightarrow p + \pi$$

is assumed to be baryon, or baryon resonance exchange, but the details of the mechanism differ in each case in two important ways. First, the photo-induced process has no initial state absorption, and all final states are summed over. Thus, the effect of absorptive corrections is expected to be much smaller than in the pion-nucleon case. Secondly, the product of the electric charge part of the electromagnetic vertex at A in Fig. 28 and the nucleon propagator will not change as the nucleon goes off-the-mass-shell, whereas form factor effects will influence the pion-nucleon case. However, even if we retain the full final state absorption factors and the form factor reductions which were used in Trefil's fit to the backward pion-nucleon scattering we are led to the prediction of an anti-nucleon or anti-baryon beam of $\sim 10^{-30}$ cm$^2$/ster-GeV at $\sim$ 15 GeV energy. Similar intensities are computed [Berman and

Drell (1966 unpublished)] for anti-baryon beams via the diffraction mechanism in Fig. 29, but these numbers are highly sensitive to the assumed form factors for the virtual ρ-nucleon or ρ-baryon vertices. These numbers should of course be understood as little better than a dimensional guide, but they lead to tremendous anti-baryon beam fluxes from accelerators such as SLAC and are therefore of some practical importance.

## ACKNOWLEDGEMENTS

We would like to thank our many colleagues for helpful discussions during the preparation of this manuscript. Part of the work was done while one of us (A.C.H.) was a member of the Rutherford High Energy Laboratory, Chilton, and the Clarendon Laboratory, Oxford, England, and the hospitality afforded during this period is gratefully acknowledged.

## LIST OF REFERENCES


1. Aachen-Berlin-Birmingham-Bonn-Hamburg-London, (IC)- München Collaboration (1965), Nuovo Cimento 35, 659.

2. Alexander, G., B. Haber, A. Shapira, and G. Yekutieli (1965). Weizmann Institute preprint.

3. Amaldi, U. and F. Selleri (1964). Nuovo Cimento 31, 360.

4. Amati, D., S. Fubini and A. Stanghellini (1962). Nuovo Cimento 26, 896.

5. Arnold, R. C. (1964). Phys. Rev. 136, B1388.

6. Arnold, R. C. (1965). Phys. Rev. 140, B1022.

7. Ashmore, A., W. H. Range, R. T. Taylor, B. M. Townes, L. Castillejo, and R. F. Peierls (1962). Nuclear Physics 36, 258.

8. Baker, M. and R. Blankenbecler (1962). Phys. Rev. 128, 415.

9. Ball, J. S. and W. R. Frazer (1965). Phys. Rev. Letters 14, 746.

10. Baltay, C., E. C. Fowler, J. Sandweiss, J. R. Sanford, H. D. Taft, B. B. Culwick, W. B. Fowler, J. K. Kopp, R. I. Louttit, R. P. Shutt, A. M. Thorndike and M. S. Webster (1962). Proc. Intern. Conf. High-Energy Nuclear Phys., Geneva, (CERN) 233.

11. Bander, M. and G. L. Shaw (1965). Phys. Rev. 139, B956.

12. Barger, V. and M. Ebel (1965). Phys. Rev. 138, B1148.

13. Bell, J. S. (1964). Phys. Rev. Letters 13, 57.

14. Berman, S. M. and S. D. Drell (1964). Phys. Rev. 133, B791.

15. Blankenbecler, R. and M. L. Goldberger (1962). Phys. Rev. 126, 766.

16. Blanpied, W. A., J. S. Greenberg, V. W. Hughes, D. C. Lu and R. C. Minehart (1963). Phys. Rev. Letters 11, 477.

17. Blanpied, W. A., J. S. Greenberg, V. W. Hughes, P. Kitching, D. C. Lu, and R. C. Minehart (1965). Phys. Rev. Letters 14, 741.

18. Blumenthal, R. B., W. L. Faissler, P. M. Joseph, L. J. Lanzerotti, F. M. Pipkin, D. G. Stairs, J. Ballam, H. DeStaebler Jr. and A. Odian (1963). Phys. Rev. Letters 11, 496.

19. Bugg, D. V. (1963). Phys. Letters 7, 365.

20. Cambridge Bubble Chamber Group (1965). Intern. Symposium on Electron and Photon Interactions, Hamburg.

21. Chamberlain, O. (1960). Proc. Annual Rochester Conf. High Energy Phys. 10, 655.

22. Chew, G. F. (1958). Phys. Rev. 112, 1380.

23. Chew, G. F. and F. E. Low (1959). Phys. Rev. 113, 1640.

24. Chew, G. F. and S. Mandelstam (1960). Phys. Rev. 119, 467.

Chew, G. F. and S. Mandelstam (1961). Nuovo Cimento 19, 752.

25. Clementel, E. and C. Villi (1956). Nuovo Cimento 4, 1207.

26. Crouch, H. R. (1964). Phys. Rev. Letters 13, 640.

27. Dalitz, R. H. (1961). Rev. Mod. Phys. 33, 471.

28. Dar, A. (1964). Phys. Rev. Letters 13, 91.

29. Dar, A., M. Kugler, Y. Dothan and S. Nussinov (1964). Phys. Rev. Letters 12, 82.

30. Dar, A. and W. Tobocman (1964). Phys. Rev. Letters 12, 511.

31. Daudin, A., M. A. Jabiol, C. Kochowski, C. Lewin, F. Selleri, S. Mongelli, A. Romano and P. Waloscheck (1963). Phys. Letters 7, 125.

32. Dietz, K.and H. Pilkuhn (1965). Nuovo Cimento 37, 1561.

33. Dietz, K. and H. Pilkuhn (1965). Nuovo Cimento 39, 928.

32. Drell, S. D. (1960). Phys. Rev. Letters 5, 278.

33. Drell, S. D. (1961). Rev. Mod. Phys. 33, 458.

34. Drell, S. D. (1965). Proc. Intern. Symposium Electron Photon Intera. High Energies, Hamburg, 71.

35. Drell, S. D. and M. Jacob (1965). Phys. Rev. 138, B1312.

36. Drell, S. D. and J. Trefil (1966). Phys. Rev. Letters (To Be Published).

37. Durand, Loyal III, and Y. T. Chiu (1964). Phys. Rev. Letters 12, 399. Erratum: Phys. Rev. Letters 13, 45.

38. Durand, L. and Y. T. Chiu (1964). Lectures in Theoretical Physics, Vol. VIIb, p. 206, Univ. Colorado Press.

39. Durand, L. and Y. T. Chiu (1965). Phys. Rev. 137, B1530.

40. Durand, L. and Y. T. Chiu (1965). Phys. Rev. 139, B646.

41. Ferrari, E. and F. Selleri (1962). Supplemento del Nuovo Cimento 24, 453.

42. Ferrari, E. and F. Selleri (1963). Nuovo Cimento 27, 1450. Erratum: Nuovo Cimento 28, 454.

43. Foley, K. J., R. S. Gilmore, R. S. Jones, S. J. Lindenbaum, W. A. Love, S. Ozaki, E. H. Willen, R. Yamada, and L.C.L. Yuan (1965). Phys. Rev. Letters 14, 862.

44. Glauber, R. J. (1959). Lectures in Theoretical Physics, Vol. I, pp. 315-414. Interscience Publishers, Inc. New York.

45. Goebel, C. (1958). Phys. Rev. Letters 1, 337.

46. Goldberger, M. L. (1955). Phys. Rev. 99, 979.

47. Goldberger, M. L. and K. M. Watson (1964). "Collision Theory". Wiley, New York.

48. Goldhaber, A. S. (1964). Phys. Rev. 135, B508.

49. Goldhaber, G., W. Chinowsky, S. Goldhaber, W. Lee and T. O'Halloran (1963). Phys. Letters 6, 62.

50. Gottfried, K. and J. D. Jackson (1964). Phys. Letters 8, 144.

51. Gottfried, K. and J. D. Jackson (1964). Nuovo Cimento 33, 309.

52. Gottfried, K. and J. D. Jackson (1964). Nuovo Cimento 34, 735.

53. Griffiths, D. and A. M. Saperstein (1965). Argonne National Laboratory preprint.

54. Hagopian, V.,W. Selove, J. Alitti, J. P. Baton, and M. Neveu-René (1965). Phys. Rev. (To Be Published).

55. Hamilton, J. and W. S. Woolcock (1963). Rev. Mod. Phys. 35, 737.

56. Heitler, W. (1944). "The Quantum Theory of Radiation." Oxford University Press, New York.

57. Högaasen, H. and J. Högaasen (1965). Nuovo Cimento 39, 941.

58. Högaasen, H. and J. Högaasen (1965). Nuovo Cimento 40A, 560.

59. Högaasen, H., J. Högaasen, R. Keyser and B.E.Y. Svensson (1965). Nuovo Cimento (To Be Published).

60. Islam, M. M. (1963). Nuovo Cimento 30, 579.

61. Islam, M. M. and R. Piñon (1963). Nuovo Cimento 30, 837.

62. Jackson, J. D. (1965). Rev. Mod. Phys. 37, 484.

63. Jackson, J. D., J. T. Donohue, K. Gottfried, R. Keyser and B.E.Y. Svensson (1965). Phys. Rev. 139, B428.

64. Jacob, M. and G. C. Wick (1959). Annals of Phys. 7, 404.

65. James, F. E. and H. L. Kraybill (1966). Phys. Rev. (To Be Published).

66. Jones, L. W. (1965). Phys. Rev. Letters 14, 186.

67. Kumar, R. C. and E. J. Squires (1965). Nuovo Cimento 40A, 756.

68. Lanzerotti, L. J., R. B. Blumenthal, D. C. Ehn, W. L. Faissler, P. M. Joseph, F. M. Pipkin, J. K. Randolph, J. S. Russell, O. G. Stairs, and J. Tannenbaum (1965). Phys. Rev. Letters 15, 210.

69. Locher, M. P. and W. Sandhas (1965). University of Bonn Preprint.

70. Omnes, R. (1965). Phys. Rev. 137, B649.

71. Orear, J., R. Rubinstein, D. B. Scarl, D. H. White, A. D. Krisch, W. R. Frisken, A. L. Read, and H. Ruderman (1965). Phys. Rev. Letters 15, 309.

72. Ringland, G. A. and R.J.N. Phillips (1964). Phys. Letters 12, 62.

73. Ross, M. H. and G. L. Shaw (1964). Phys. Rev. Letters 12, 627.

74. Saclay-Orsay-Bari- Bologna Collaboration (1964). Nuovo Cimento 29, 515.

75. Saclay-Orsay-Bari-Bologna Collaboration (1964). Intern. Conf. High-Energy Phys., Dubna, Abstract VII – 42.

76. Selleri, F. (1964). Lectures in Theoretical Physics, Vol VIIb, Univ. Colorado Press.

77. Shaw, G. L. and D. Y. Wong (1963). Phys. Rev. 129, 1379.

78. Sopkovich, N. J. (1962). Dissertation, Carnegie Inst. of Tech. (Unpublished).

79. Sopkovich, N. J. (1962). Nuovo Cimento 26, 186.

80. Squires, E. J. (1964). Nuovo Cimento 34, 1328.

81. Squires, E. J. (1965). Nuovo Cimento 39, 300.

82. Squires, E. J. (1965). Nuovo Cimento (To Be Published).

83. Stodolsky J. and J. J. Sakurai (1963). Phys. Rev. Letters 11, 90.

84. Svensson, B.E.Y. (1965). Nuovo Cimento 37, 714.

85. Svensson, B.E.Y. (1965). Nuovo Cimento 39, 66.

86. Trefil. J. (1966). Bulletin of the American Phys. Society 11, 23. Phys. Rev. (To Be Published).

87. Treiman, S. B. and C. N. Yang (1962). Phys. Rev. Letters 8, 140.

88. Watson, H.D.D. (1965). Phys. Letters 17, 72.

89. Wigner, E. P. (1955). Annals of Math. 62, 548.

FIGURE CAPTIONS

1. Nucleon exchange diagrams for pion-nucleon scattering.
2. One-pion exchange contribution to elastic nucleon-nucleon scattering.
3. Singularities in amplitude for elastic nucleon-nucleon scattering.
4. One-pion exchange contribution to the process $\pi + N \rightarrow \pi + \pi + N$.
5. One-pion exchange contribution to the process $\pi + N \rightarrow \pi + \pi + (n)$, where (n) denotes an arbitrary final state of two or more particles.
6. Coordinate system in the frame, O, of zero total momentum for the pions produced in the reaction $\pi + N \rightarrow \pi + \pi + N$. $\underset{\sim}{p}$ is the momentum of one of the final state pions, $\underset{\sim}{\hat{n}}$ is perpendicular to the nucleon scattering plane and $\underset{\sim}{p}_{\pi}$ is the momentum of the incident pion as seen in O.
7. One-pion-exchange contribution to pion production of a $\rho$ meson.
8. Initial and final state interaction corrections for the one-pion exchange contribution to the process $\pi + N \rightarrow \pi + \pi + N$.
9. Distribution of $-t/\mu^2$ for the processes: a) $\pi^- + p \rightarrow \pi^- + \pi^0 + p$; b) $\pi^- + p \rightarrow \pi^- + \pi^+ + n$ [taken from SOBB Collaboration (1963)].
10. Comparison of experimental data for the process $\bar{p} + p \rightarrow \bar{\Lambda} + \Lambda$ and the fit of Dar (1964). The theoretical curves were normalized to give correctly the number of events in the first interval of the experimental histogram. [Taken from Dar (1964)].
11. Comparison of experimental data for the process $K^+ p \rightarrow K^* N^*$ and the theoretical fit of Dar (1964). The experimental data was taken from Goldhaber et al (1963). The calculation of the one-pion exchange curve is due to Berman as quoted in this reference [taken from Dar (1964)].

12. Spin density matrix elements for the $\rho^-$ in the process $\pi^- + p \rightarrow \rho^- + p$ taken from Hagopian et al (1965). The curves give the theoretical predictions of the absorption model at 2.75 GeV/c as quoted in this reference. The t scale is given for 2.88 GeV/c and for $M_{\pi\pi}$ = 765 MeV.

13. Final state interaction corrections for the one-pion exchange contribution to the process $\gamma + p \rightarrow \rho + p$.

14. Comparison of theory and experiment for the process $\pi^+ + p \rightarrow \rho^+ + p$ at 2.75 GeV/c taken from Jackson (1965). The histogram represents the data of SOBB Collaboration (1965) as quoted in this reference.

15. The total cross-section for the processes $\pi^\pm + p \rightarrow \rho^\pm + p$ as a function of incident pion momentum taken from Jackson et al (1965). The upper (lower) solid curve is a fit for $\pi^+(\pi^-)$ assuming only one-pion exchange with absorption corrections, the difference being caused by different absorption effects. The dashed curve is the cross-section fit with the Amaldi-Selleri (1964) form factor.

16. Angular distributions in cos $\theta$ and $\Phi$ for the decay products $K^o$ and $\pi^+$ from the resonance $K^*$ produced in the process $K^+ + p \rightarrow K^* + p$ at 3 GeV/c. The angles are as defined in the text. [Taken from Jackson (1965)] .

17. Theoretical and experimental $K^*$ density matrix elements for the process $K^+ + p \rightarrow K^* + p$ at 3 GeV/c from Jackson et al (1965). The solid and dashed curves refer to different values for the vector meson coupling constants as described in this reference.

18. Comparison of absorption model fit with experiment for the differential cross-section of the process in Fig. 17. The solid and dashed curves correspond to those of Fig. 17. [From Jackson et al (1965)] .

19. Absorption model fit to the process $K^+ + p \rightarrow K^* + p$ at 5 GeV/c taken from Jackson et al (1965). The curves are calculated with the same coupling constants as those of Fig. 18.

20. Diagrammatic representation of one-channel K-matrix equations.

21 K-matrix fit to $\bar{K}N$ charge exchange cross-section for 1.80 GeV/c beam momentum. [Taken from Arnold (1964)] .

22. t-channel ladder approximation for a "Reggeized" $\rho$ exchange K-matrix element.

23. One-pion-exchange contribution to photoproduction of a charged pion beam.

24. Comparison of experimental results for $\pi^-$ photoproduction from beryllium with predictions of the one-pion-exchange calculation [taken from Blumenthal et al (1963)] .

25. Coherent diffraction photoproduction of $\rho^o$ followed by decay into pions.

26. Comparison of one-pion-exchange and diffraction scattering fit to pion photoproduction from beryllium. [N. Hicks (1965 unpublished)] . The experimental data are taken from Blumenthal et al (1963).

27. $K^*$ exchange contribution to photoproduction of a $K^o$ beam in the process $\gamma + p \rightarrow k^o + \Sigma^+$.

28. Nucleon exchange contribution to photoproduction of an antiproton beam.

29. Coherent diffraction photoproduction of $\rho^o$ followed by decay into a proton-antiproton pair.

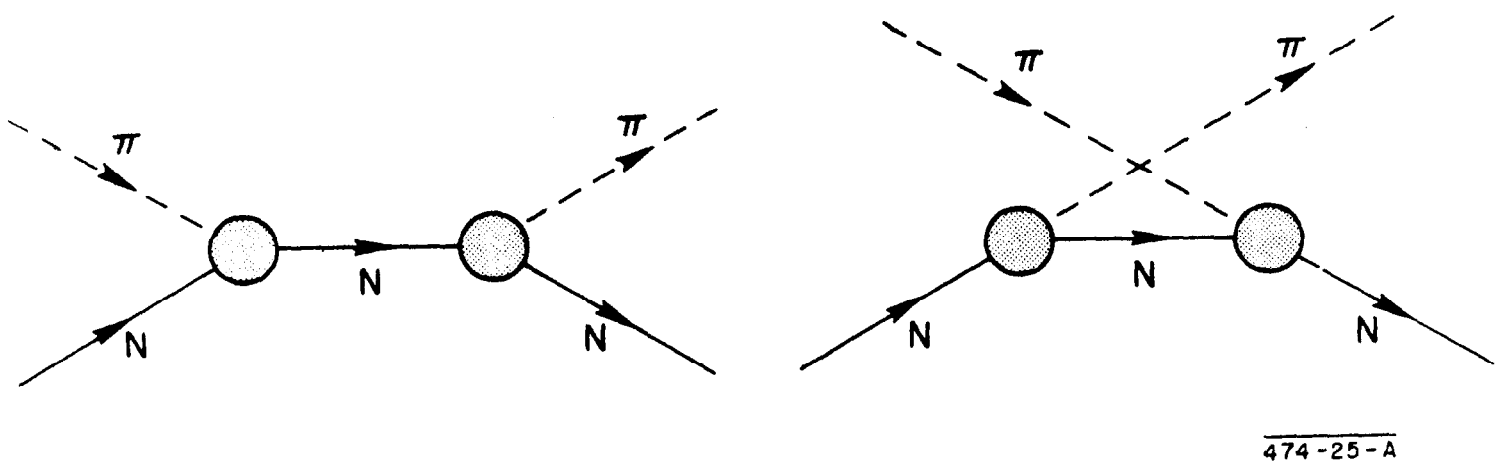


474-25-A

Fig. 1

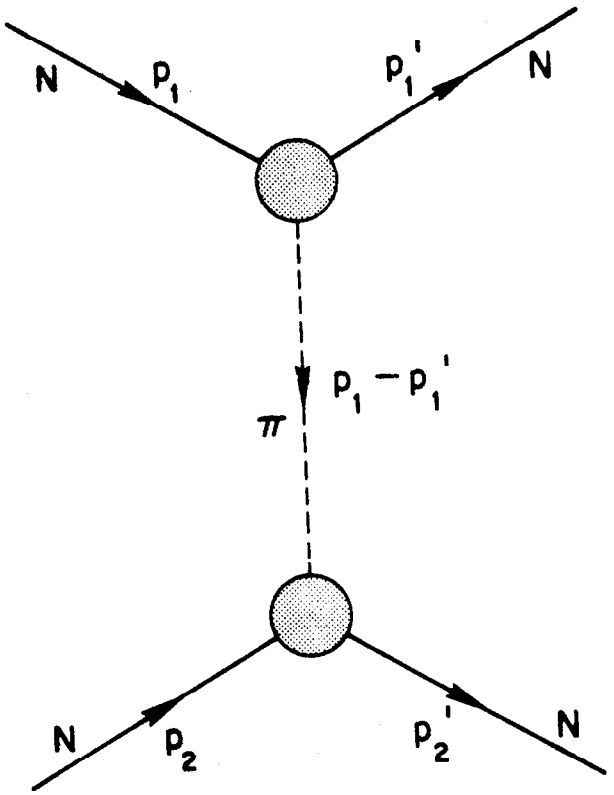


474-6-A

Fig. 2

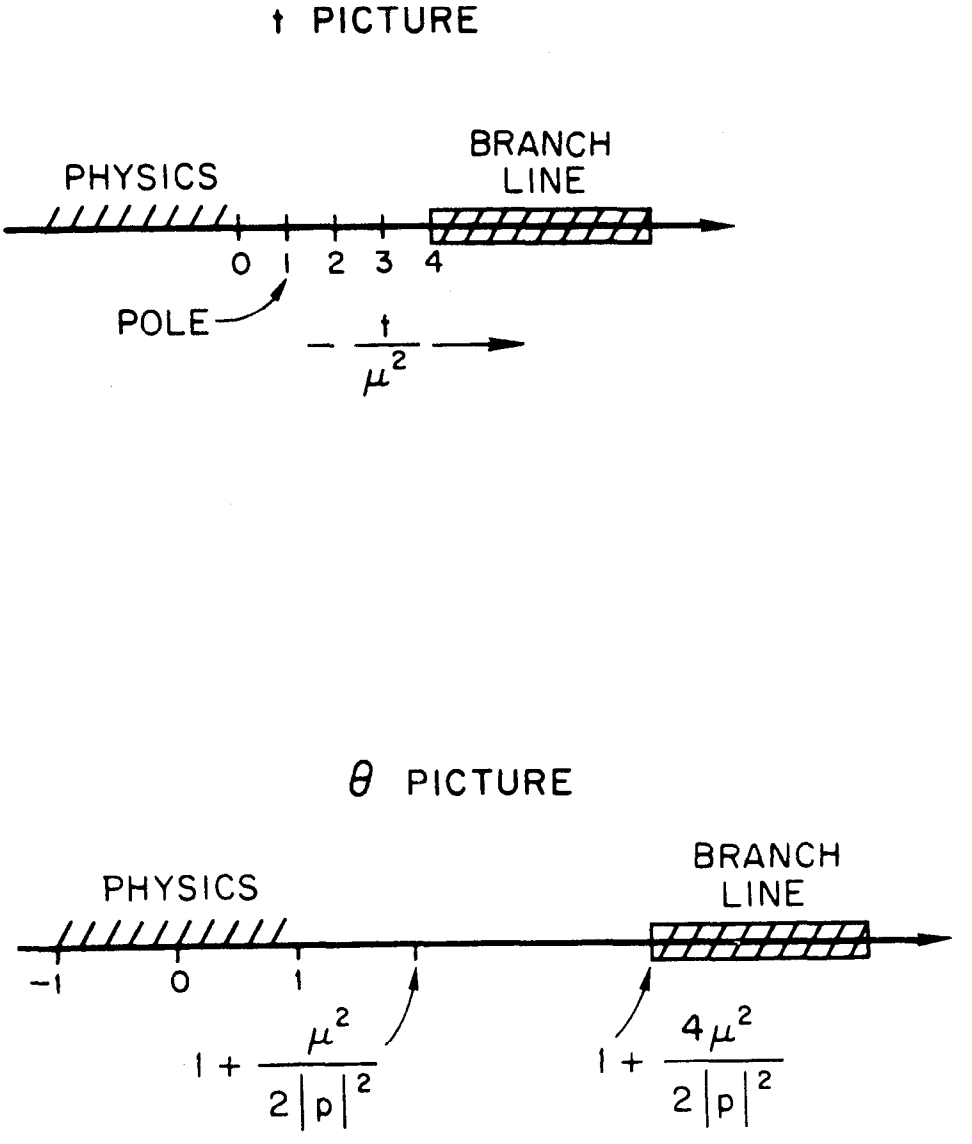
t PICTURE
PHYSICS
BRANCH LINE
0 1 2 3 4
POLE
$-\frac{t}{\mu^2}$
θ PICTURE
PHYSICS
BRANCH LINE
-1 0 1
$1+\frac{\mu^2}{2|p|^2}$
$1+\frac{4\mu^2}{2|p|^2}$

474-5-A

Fig. 3

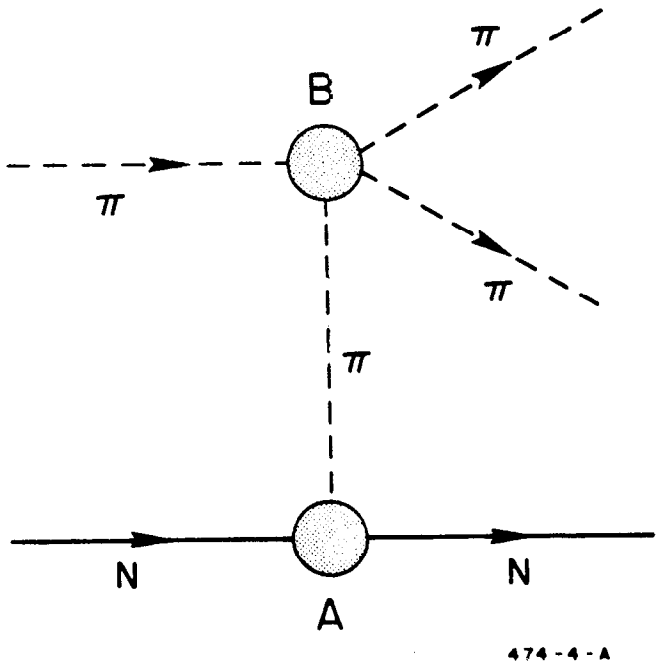


Fig. 4

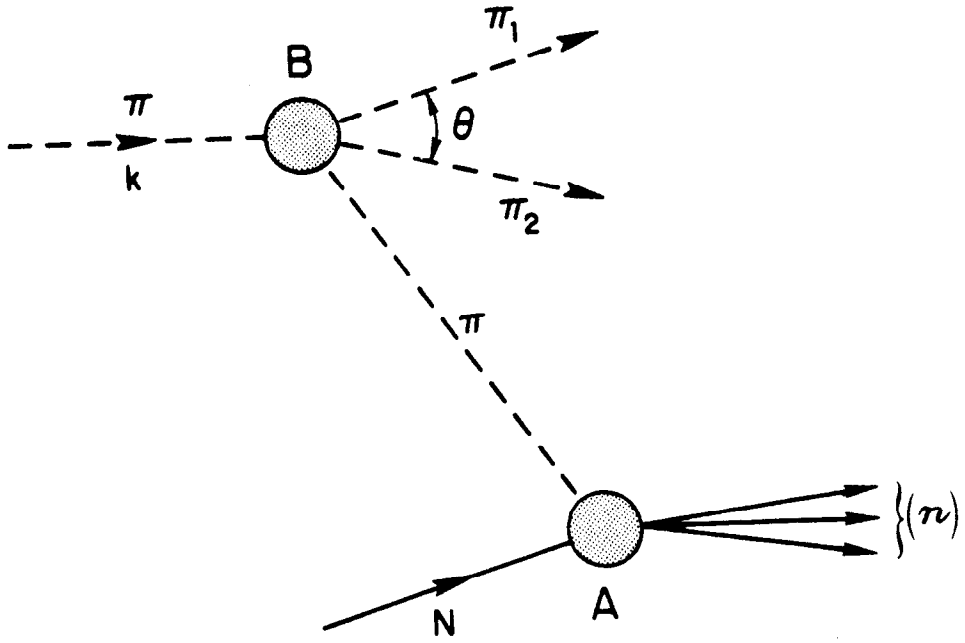


Fig. 5

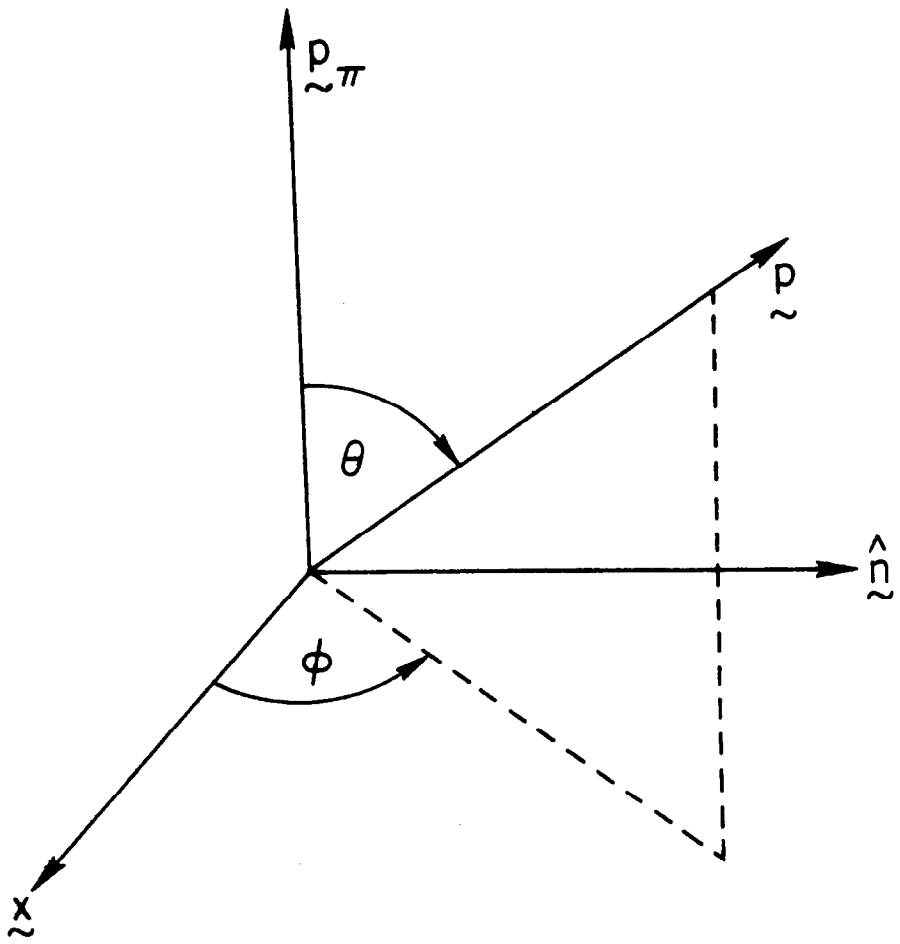
$\underset{\sim}{p}_{\pi}$
$\underset{\sim}{p}$
$\theta$
$\hat{\underset{\sim}{n}}$
$\phi$
$\underset{\sim}{x}$

474-10-A

Fig. 6

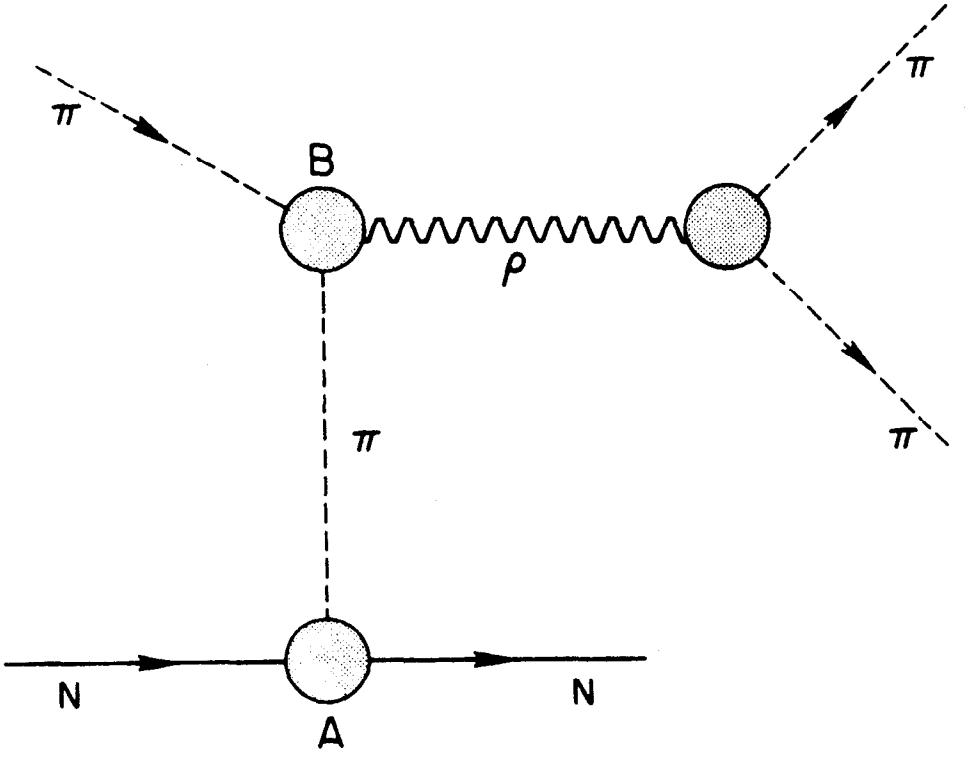


Fig. 7

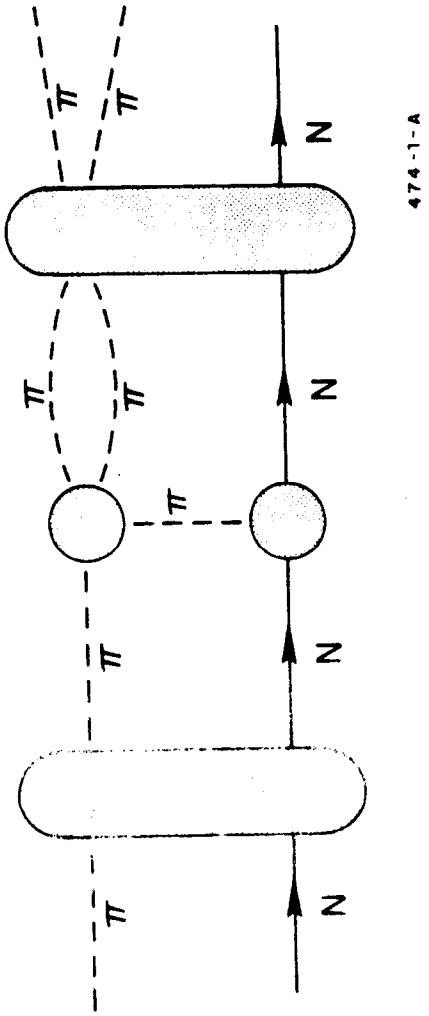


Fig. 8

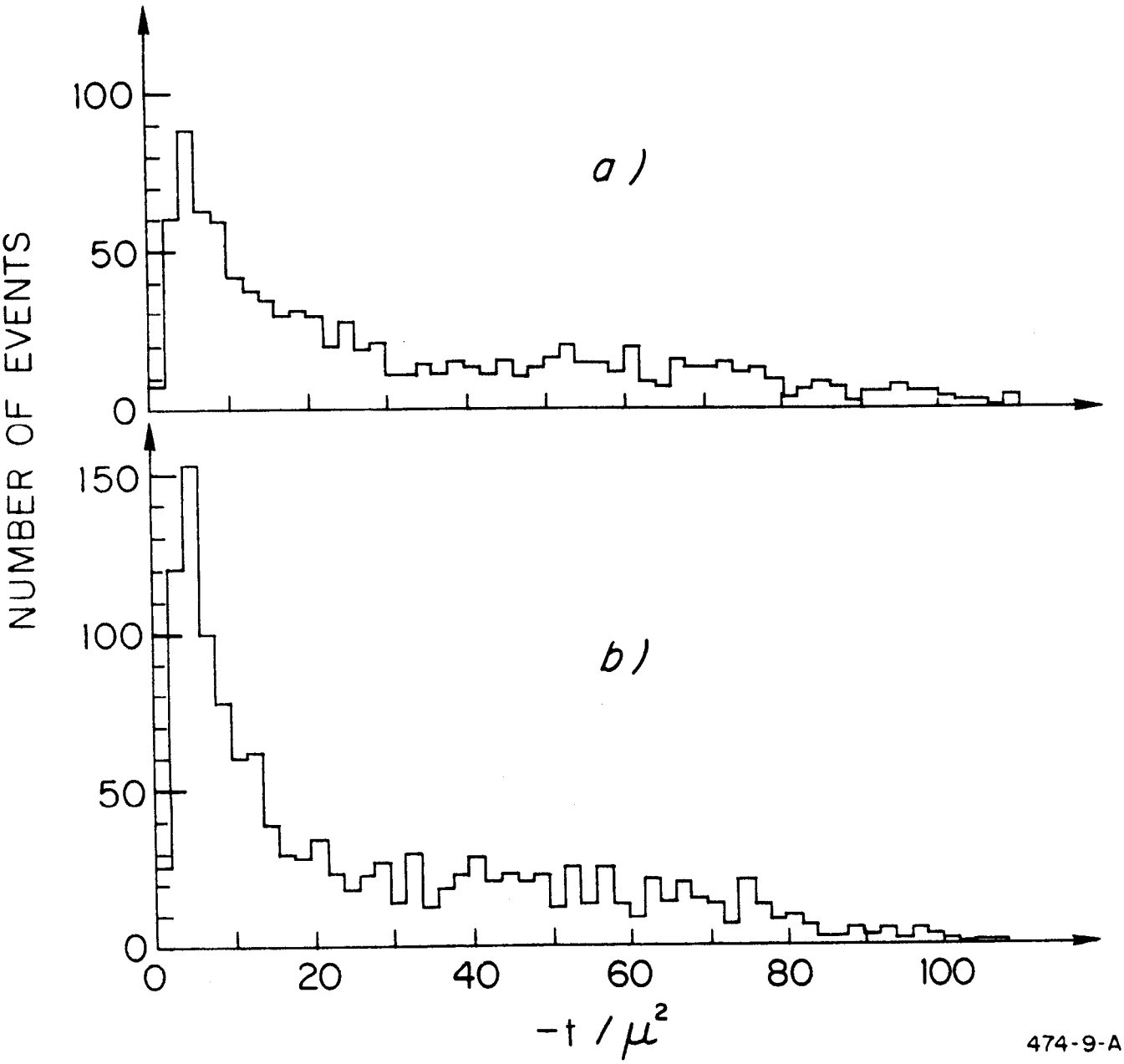
NUMBER OF EVENTS
100
50
0
a)
150
100
50
0
b)
0
20
40
60
80
100
$-t/\mu^2$
474-9-A

Fig. 9

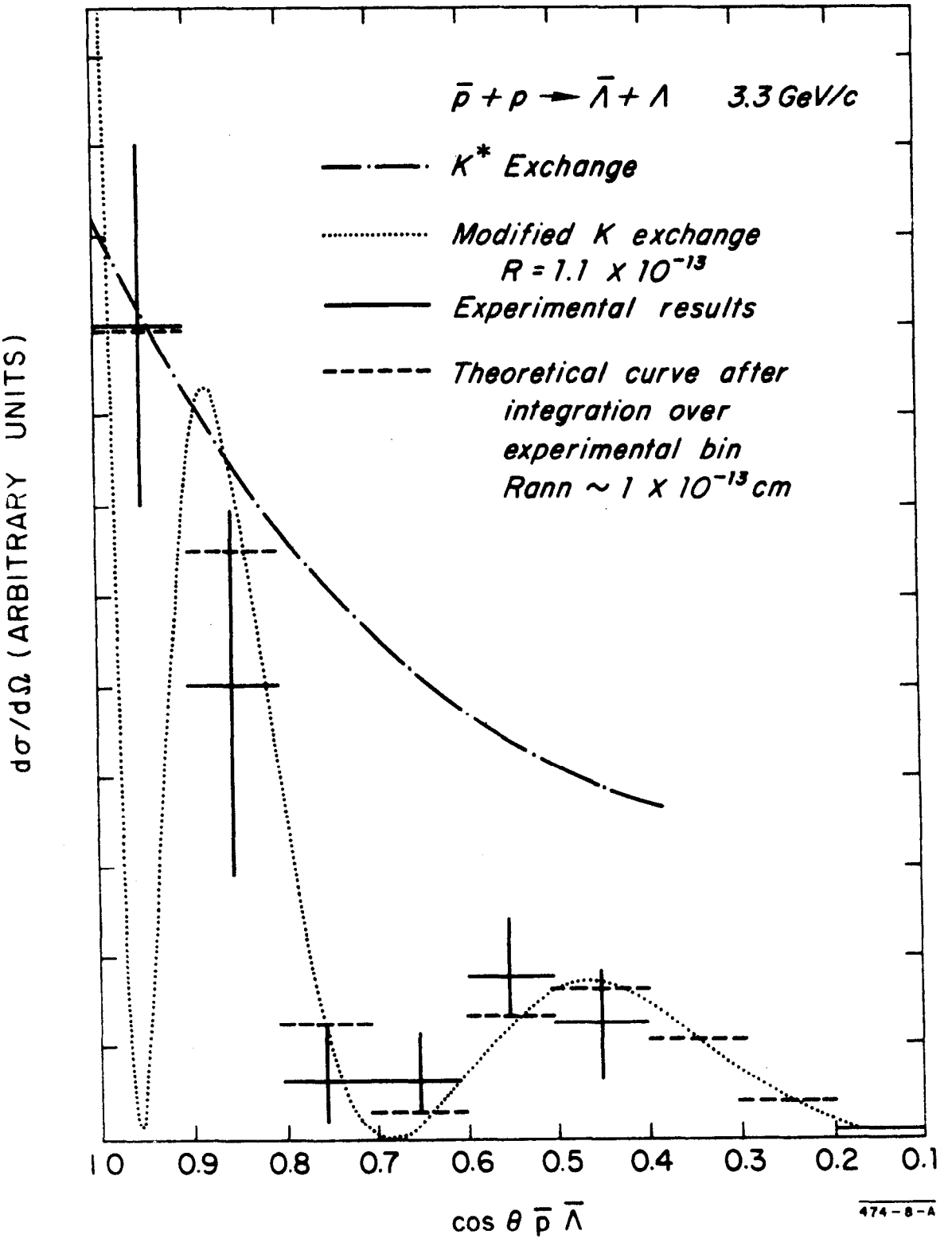
$\bar{p} + p \rightarrow \bar{\Lambda} + \Lambda$ 3.3 GeV/c
$K^*$ Exchange
Modified K exchange
$R = 1.1 \times 10^{-13}$
Experimental results
Theoretical curve after integration over experimental bin
$R_{ann} \sim 1 \times 10^{-13}$ cm
$d\sigma/d\Omega$ (ARBITRARY UNITS)
1.0 0.9 0.8 0.7 0.6 0.5 0.4 0.3 0.2 0.1
$\cos\theta\ \bar{p}\ \bar{\Lambda}$
474-8-A

Fig. 10

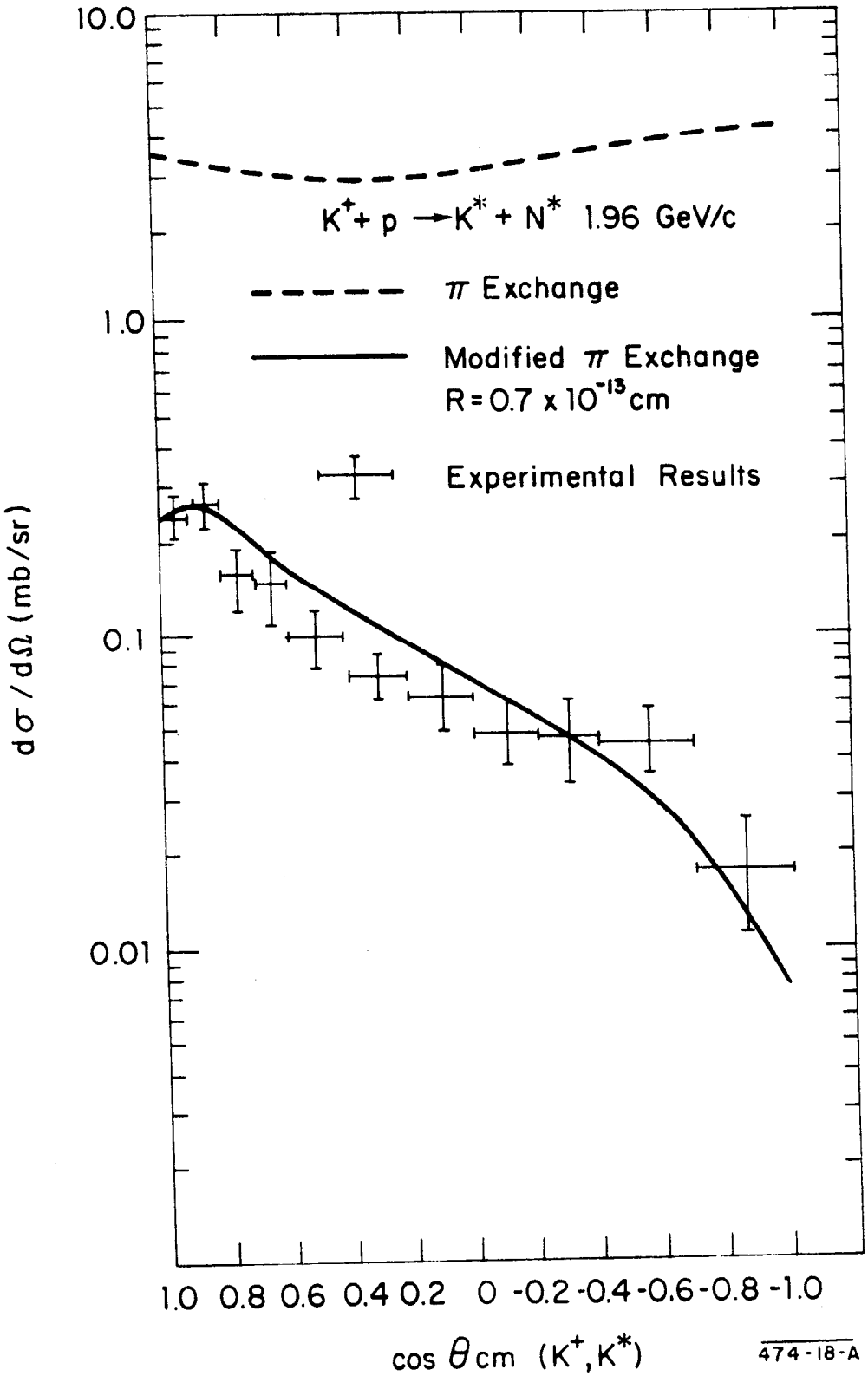
10.0
1.0
0.1
0.01
$K^+ + p \rightarrow K^* + N^*$ 1.96 GeV/c
$\pi$ Exchange
Modified $\pi$ Exchange
$R = 0.7 \times 10^{-13}$ cm
Experimental Results
$d\sigma / d\Omega$ (mb/sr)
1.0 0.8 0.6 0.4 0.2 0 -0.2 -0.4 -0.6 -0.8 -1.0
$\cos\theta$ cm $(K^+, K^*)$
474-18-A

Fig. 11

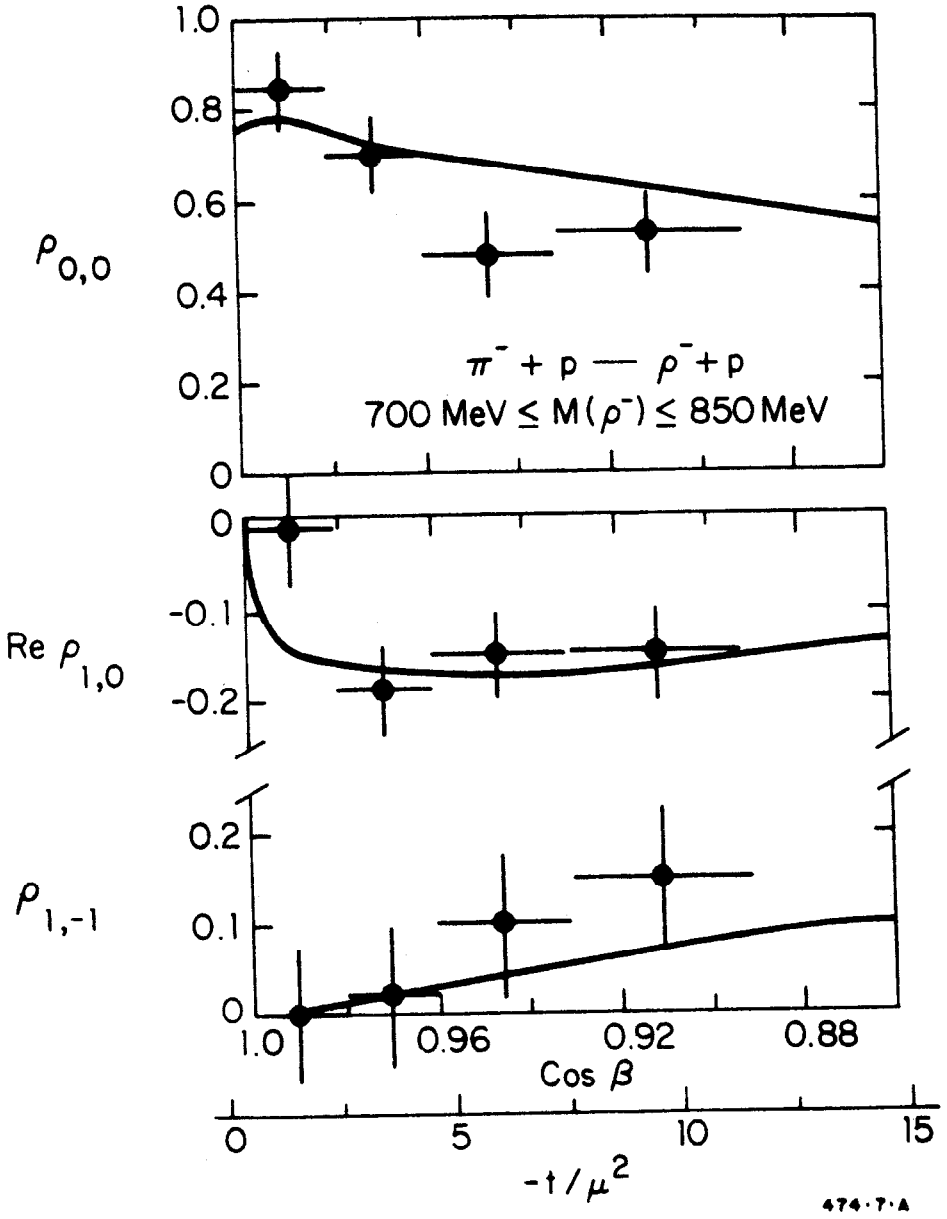
1.0
0.8
0.6
0.4
0.2
0
$\rho_{0,0}$
$\pi^- + p \rightarrow \rho^- + p$
700 MeV ≤ M($\rho^-$) ≤ 850 MeV
0
-0.1
-0.2
Re $\rho_{1,0}$
0.2
0.1
0
$\rho_{1,-1}$
1.0
0.96
0.92
0.88
Cos $\beta$
0
5
10
15
$-t/\mu^2$
474-7-A

Fig. 12

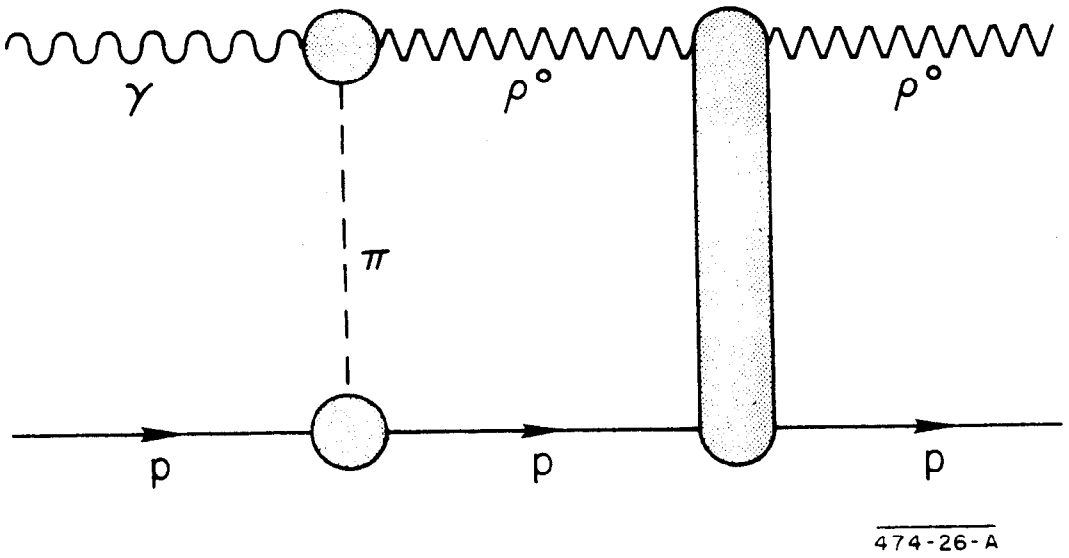


Fig. 13

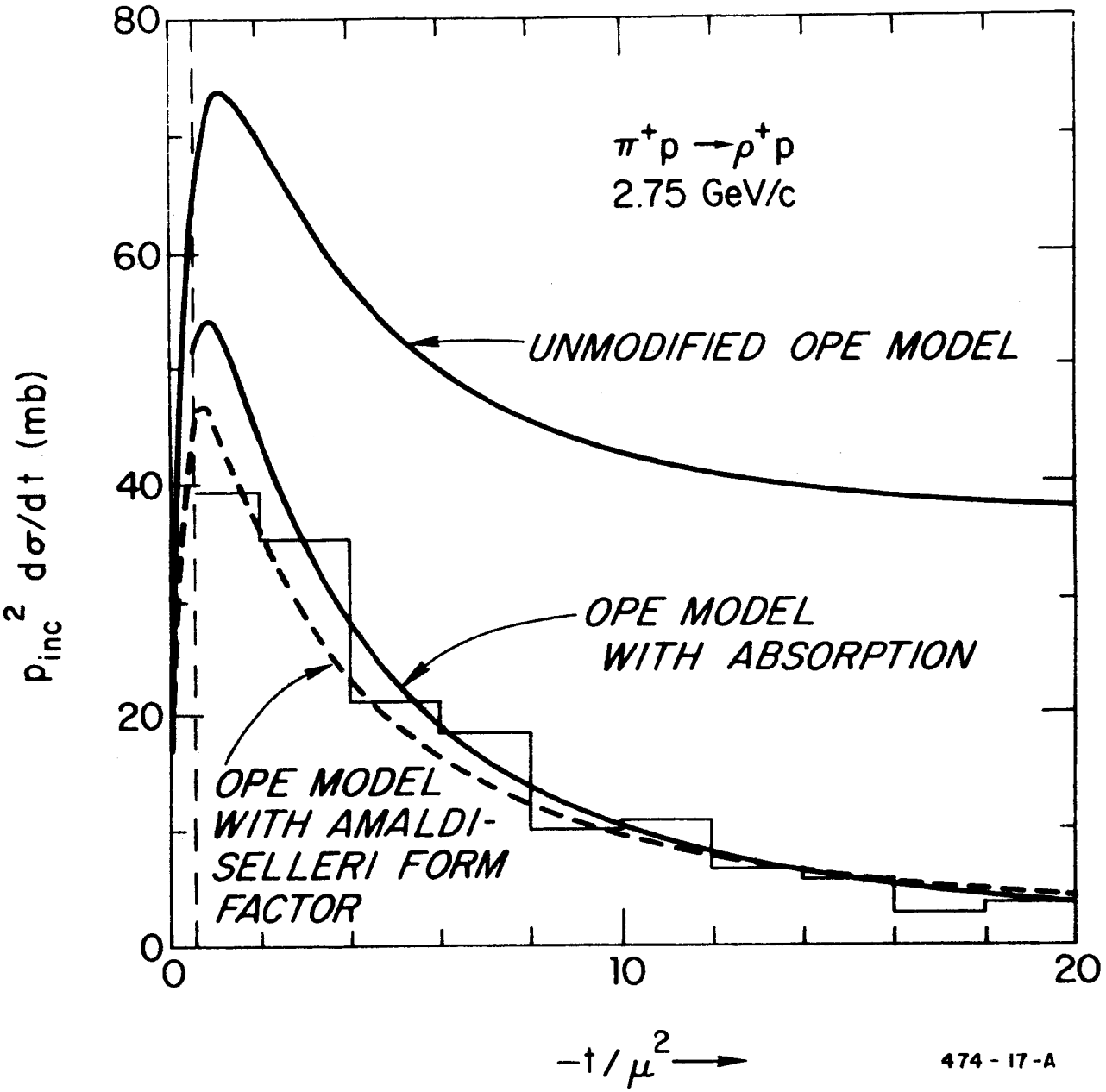
80
60
40
20
0
0
10
20
$\pi^+ p \rightarrow \rho^+ p$
2.75 GeV/c
UNMODIFIED OPE MODEL
OPE MODEL
WITH ABSORPTION
OPE MODEL
WITH AMALDI-
SELLERI FORM
FACTOR
$p_{inc}^2 \, d\sigma/dt$ (mb)
$-t/\mu^2 \rightarrow$
474 - 17 - A

Fig. 14

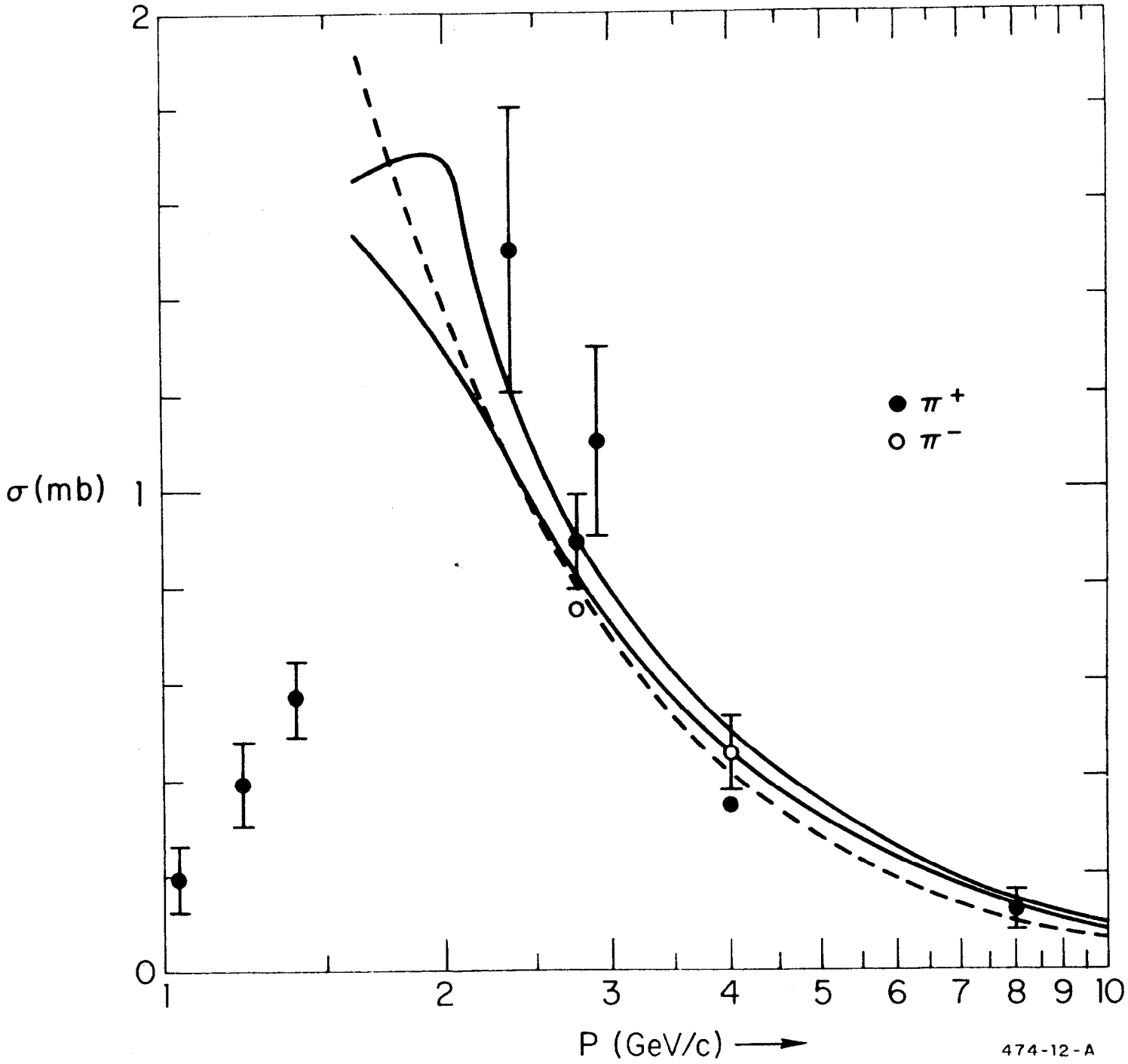


Fig. 15

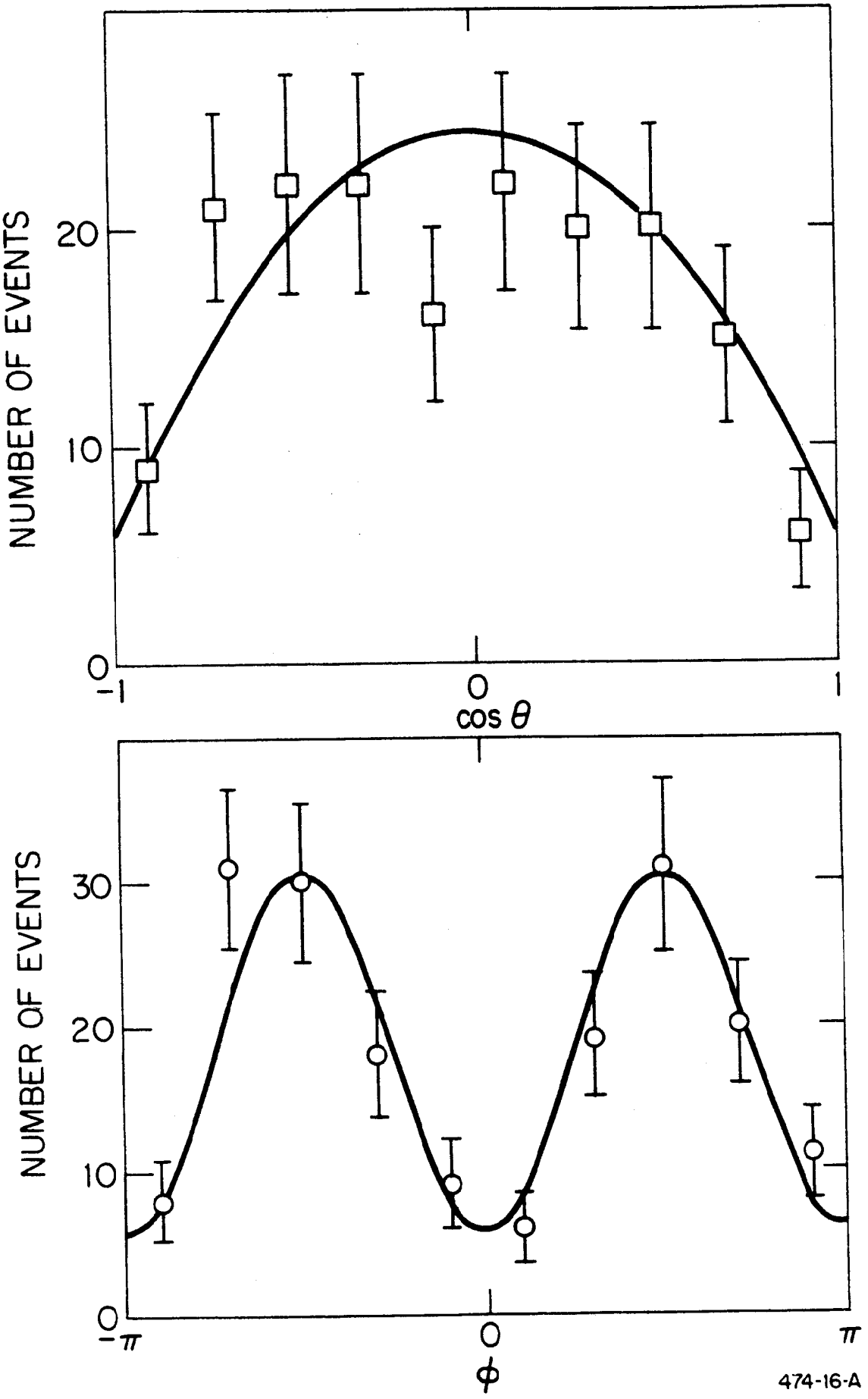
NUMBER OF EVENTS
20
10
0
-1
0
1
cos θ
NUMBER OF EVENTS
30
20
10
0
-π
0
π
φ
474-16-A

Fig. 16

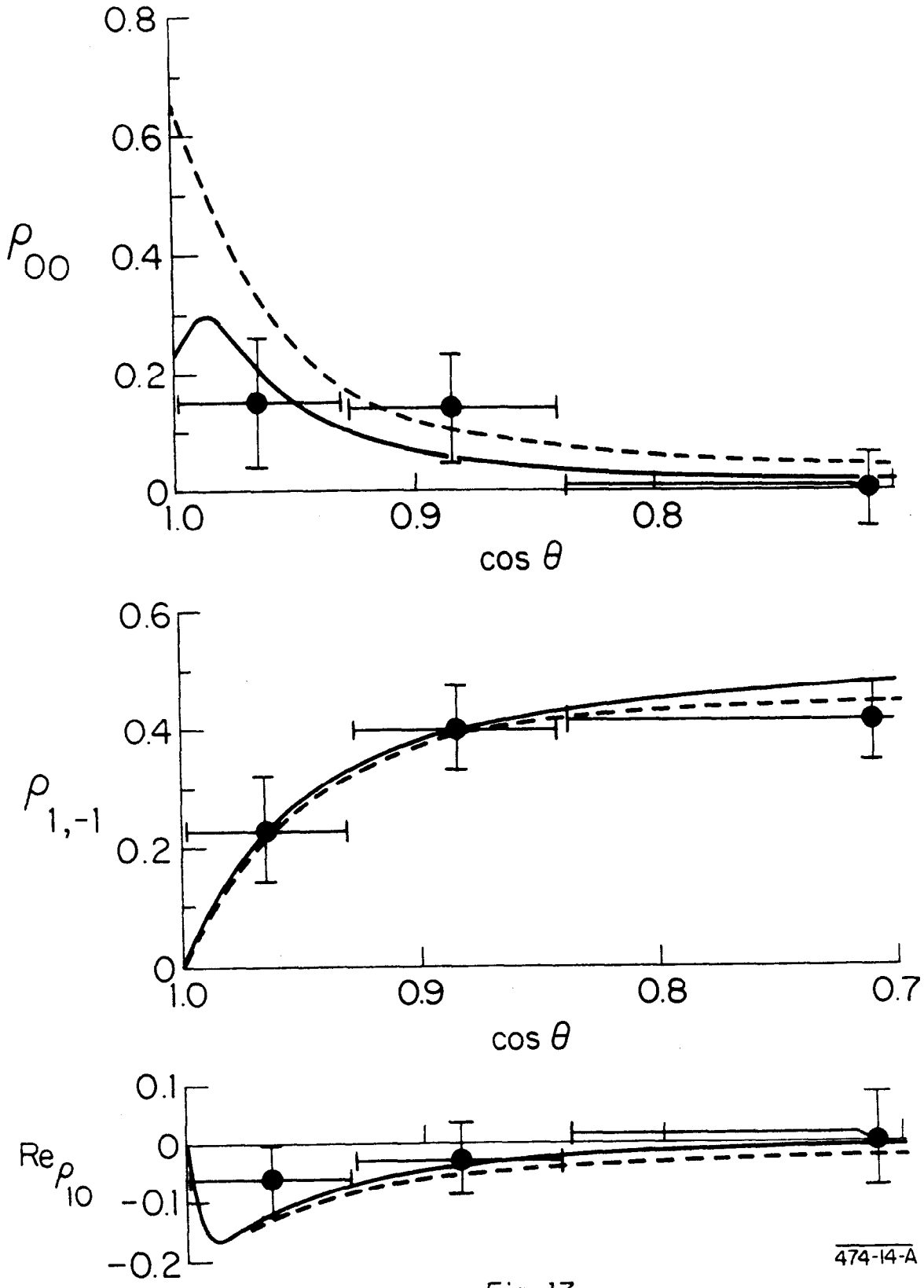
0.8
0.6
$\rho_{00}$
0.4
0.2
0
1.0
0.9
0.8
cos θ
0.6
0.4
$\rho_{1,-1}$
0.2
0
1.0
0.9
0.8
0.7
cos θ
0.1
0
$\mathrm{Re}\rho_{10}$
-0.1
-0.2
474-14-A

Fig. 17

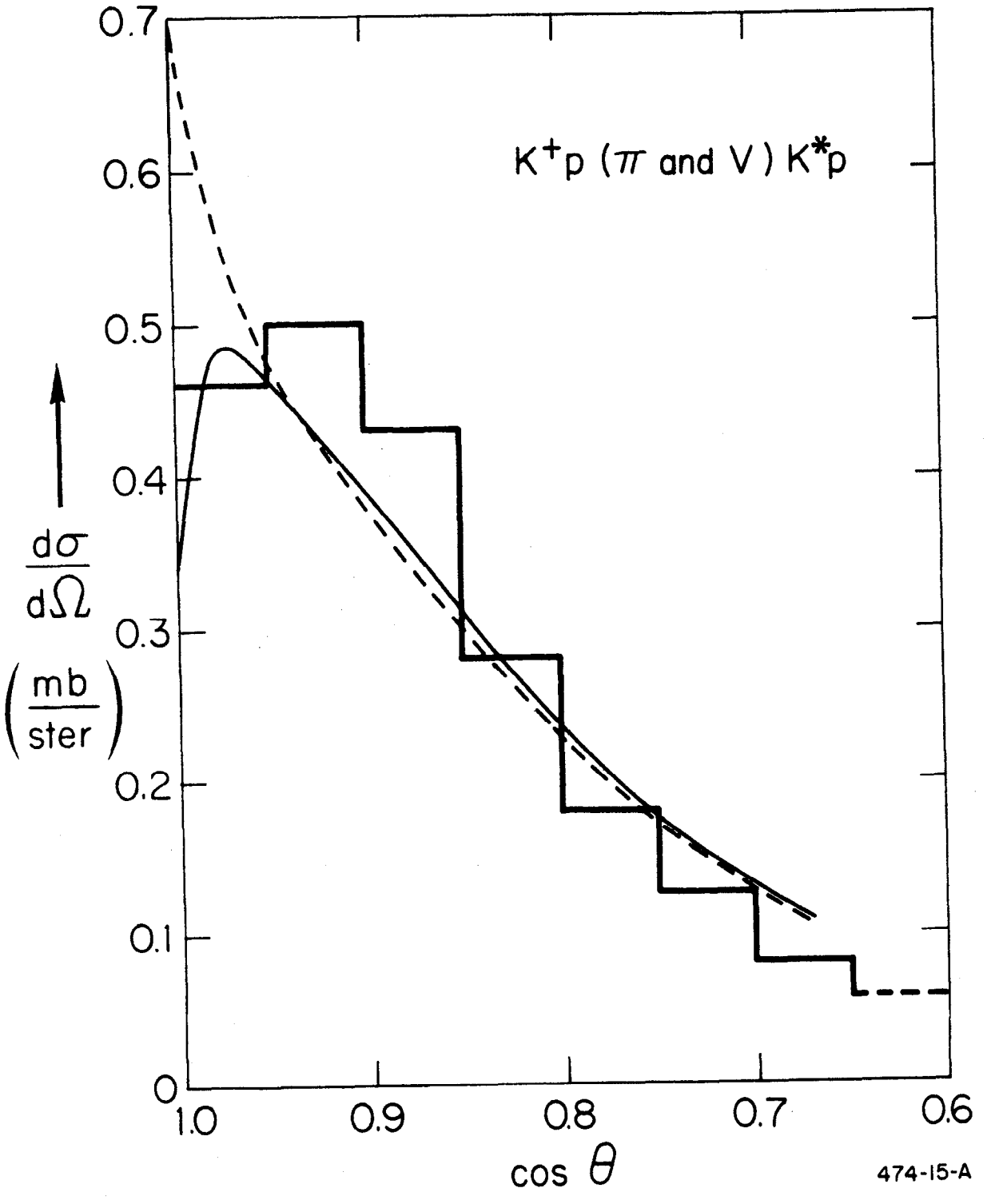
$K^+p$ ($\pi$ and V) $K^*p$
0.7
0.6
0.5
0.4
0.3
0.2
0.1
0
$\frac{d\sigma}{d\Omega}$ $\left(\frac{mb}{ster}\right)$
1.0
0.9
0.8
0.7
0.6
cos $\theta$
474-15-A

Fig. 18

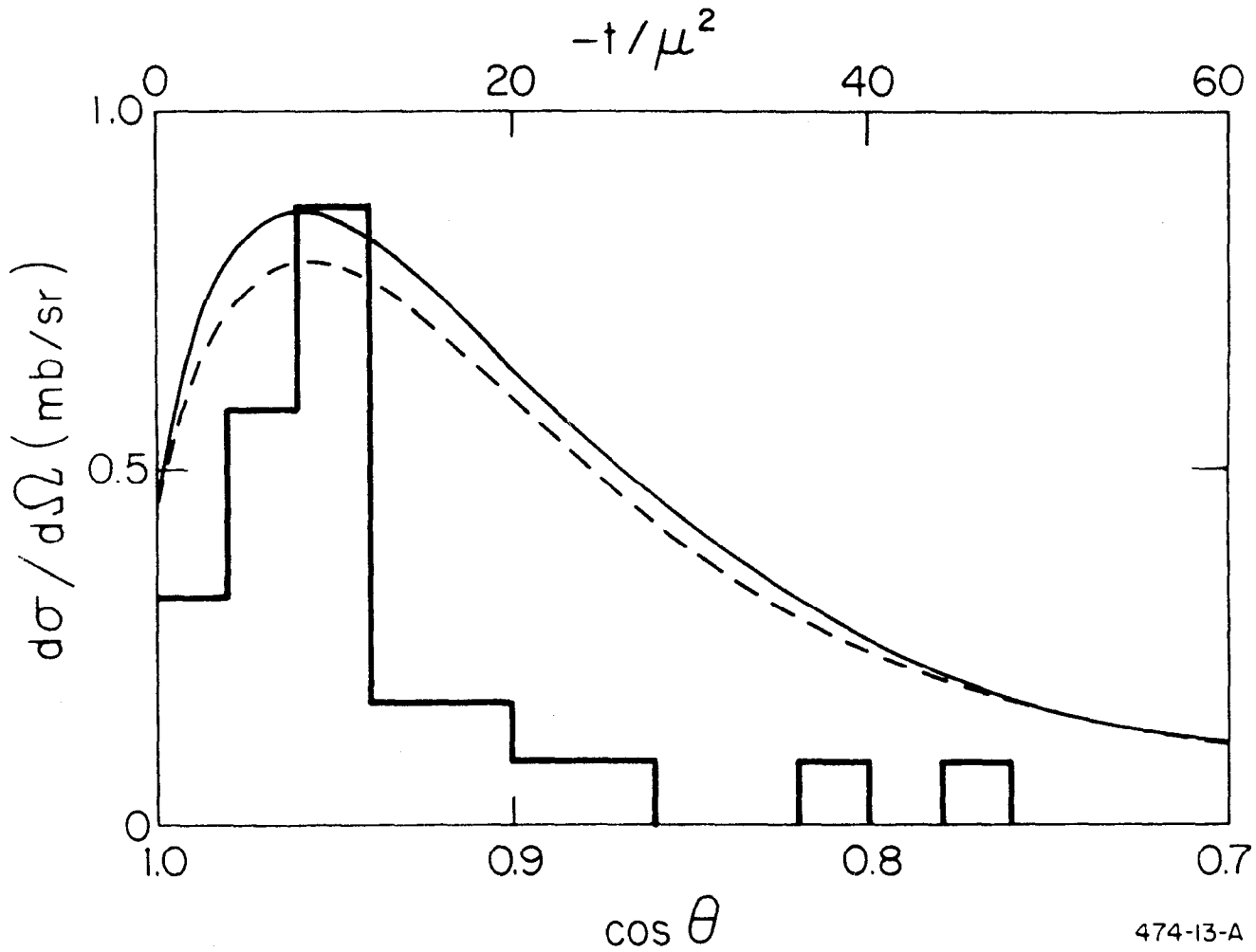
$-t/\mu^2$
0
20
40
60
1.0
0.5
0
$d\sigma/d\Omega$ (mb/sr)
1.0
0.9
0.8
0.7
cos $\theta$
474-13-A

Fig. 19

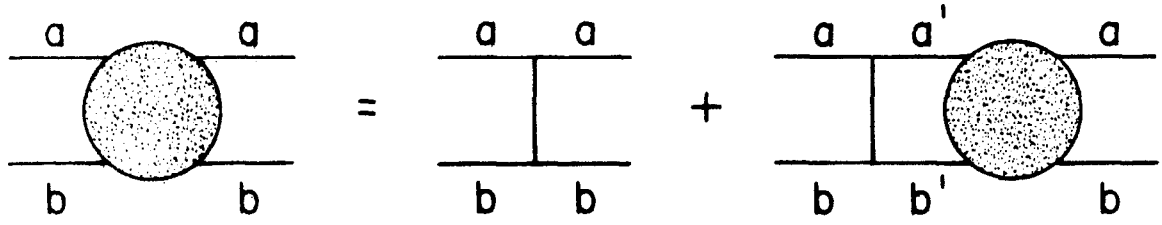


T = B + iBT

a.)

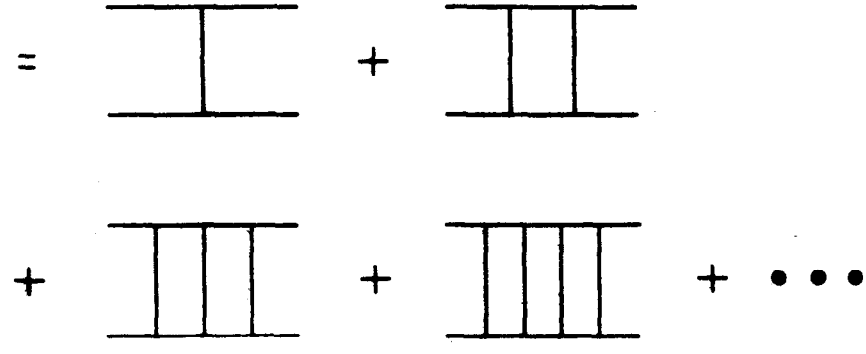


b.)

474 - 29 - A

Fig. 20

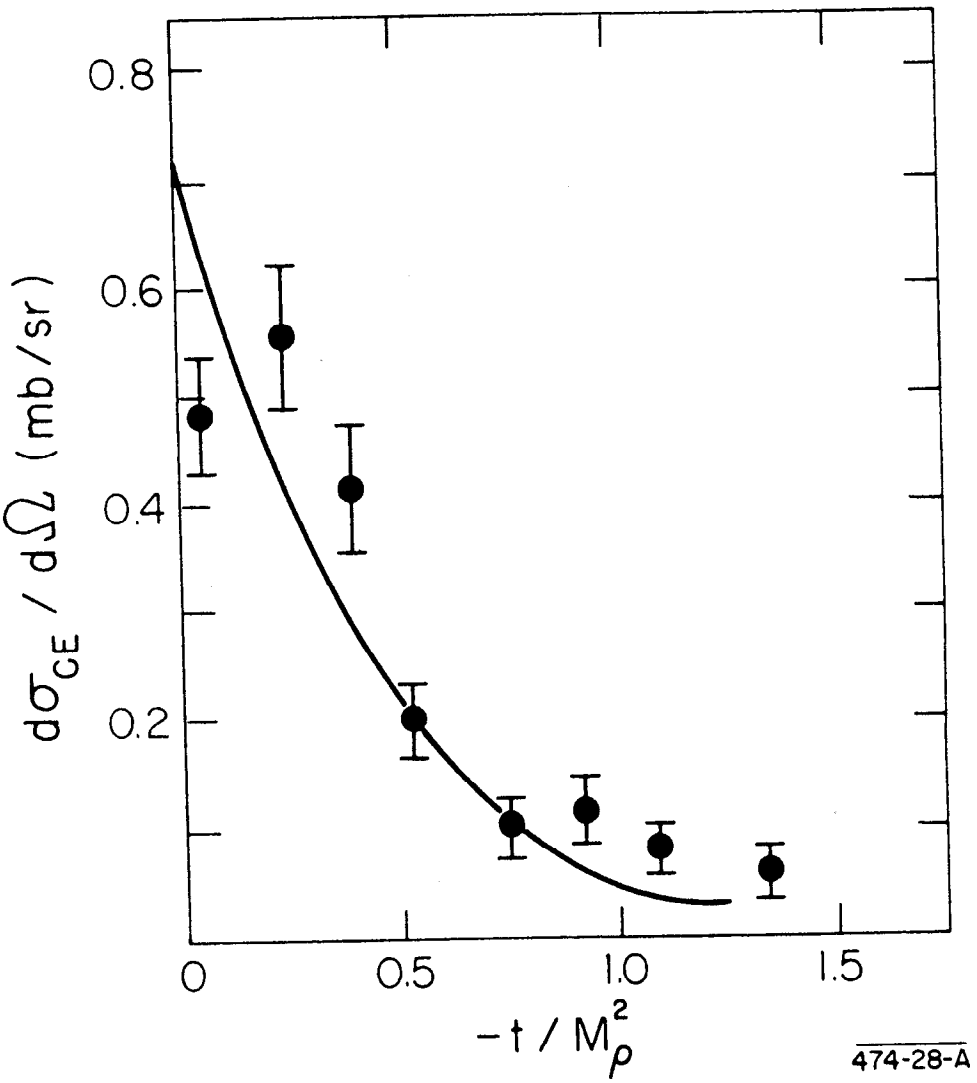


Fig. 21

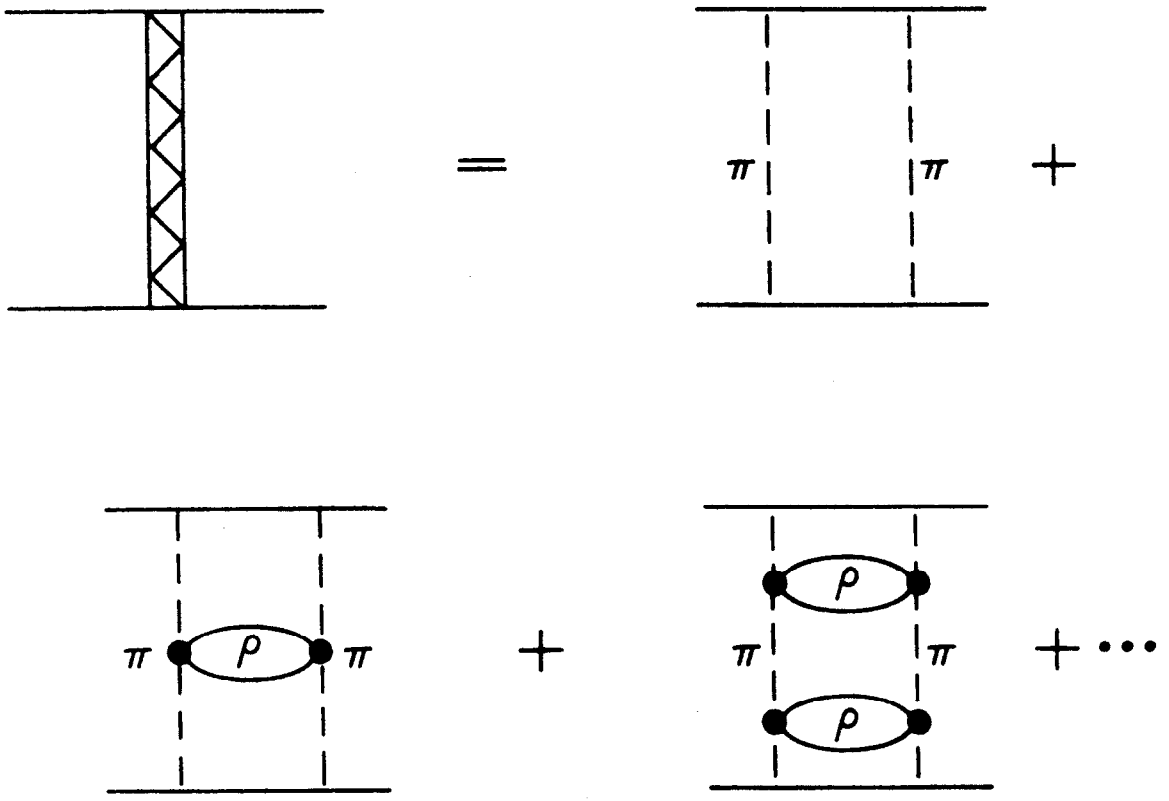


474-27-A

Fig. 22

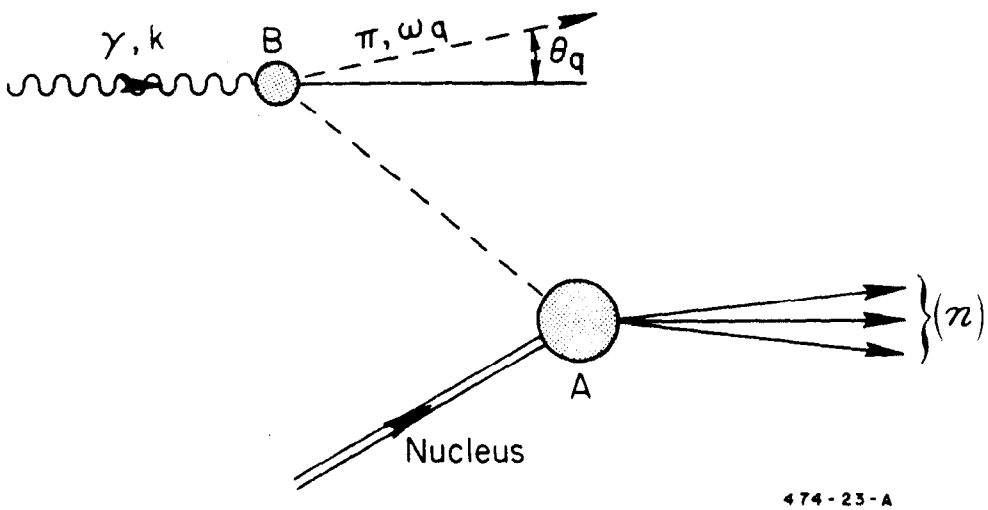


Fig. 23

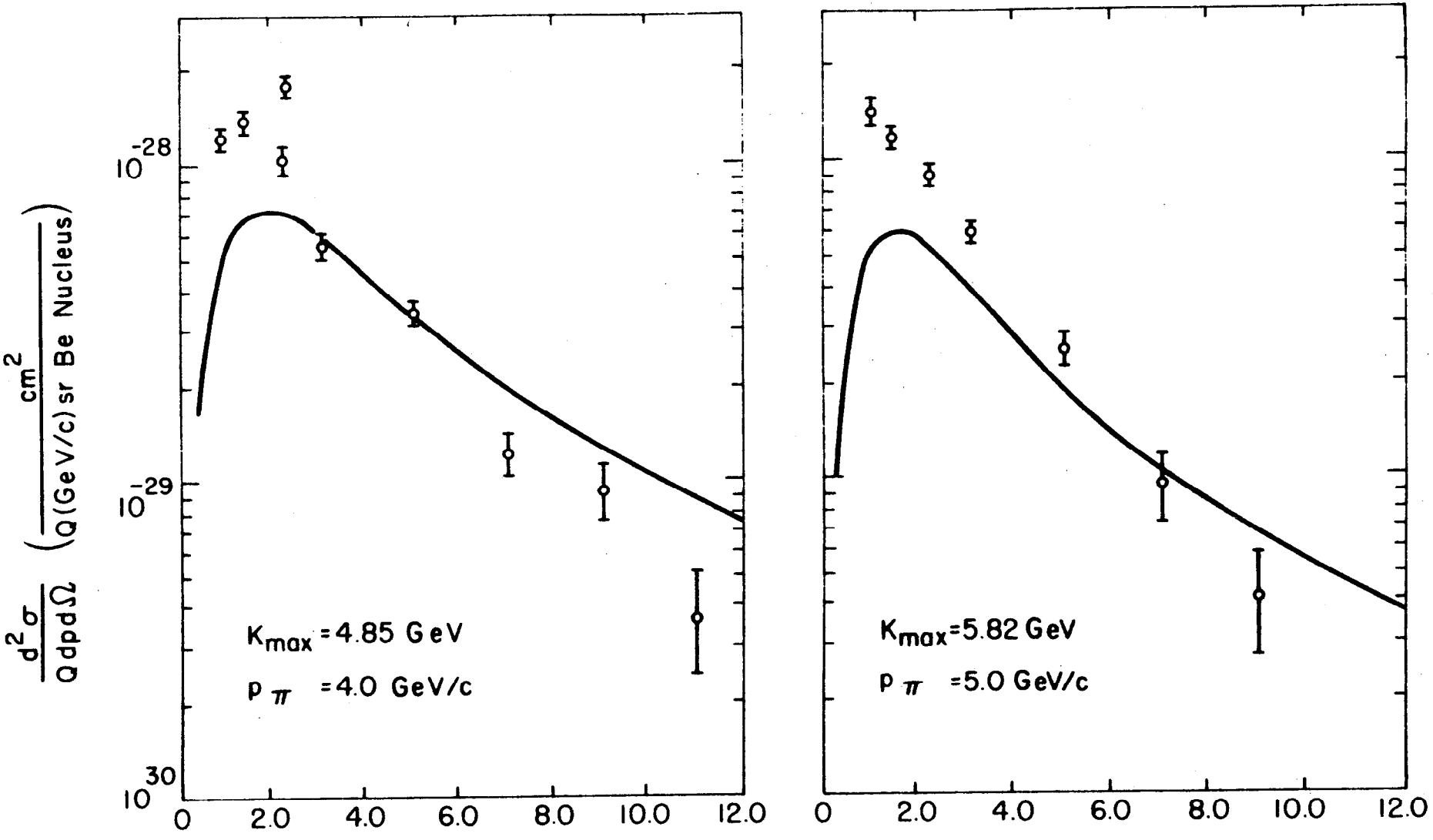
$\frac{d^2\sigma}{Q dp d\Omega}$ $\left(\frac{cm^2}{Q(GeV/c)\,sr\ Be\ Nucleus}\right)$
$10^{-28}$
$10^{-29}$
$10^{-30}$
$K_{max}$ = 4.85 GeV
$p_\pi$ = 4.0 GeV/c
$K_{max}$ = 5.82 GeV
$p_\pi$ = 5.0 GeV/c
0
2.0
4.0
6.0
8.0
10.0
12.0
LABORATORY ANGLE IN DEGREES
312-3-A

FIG. 24

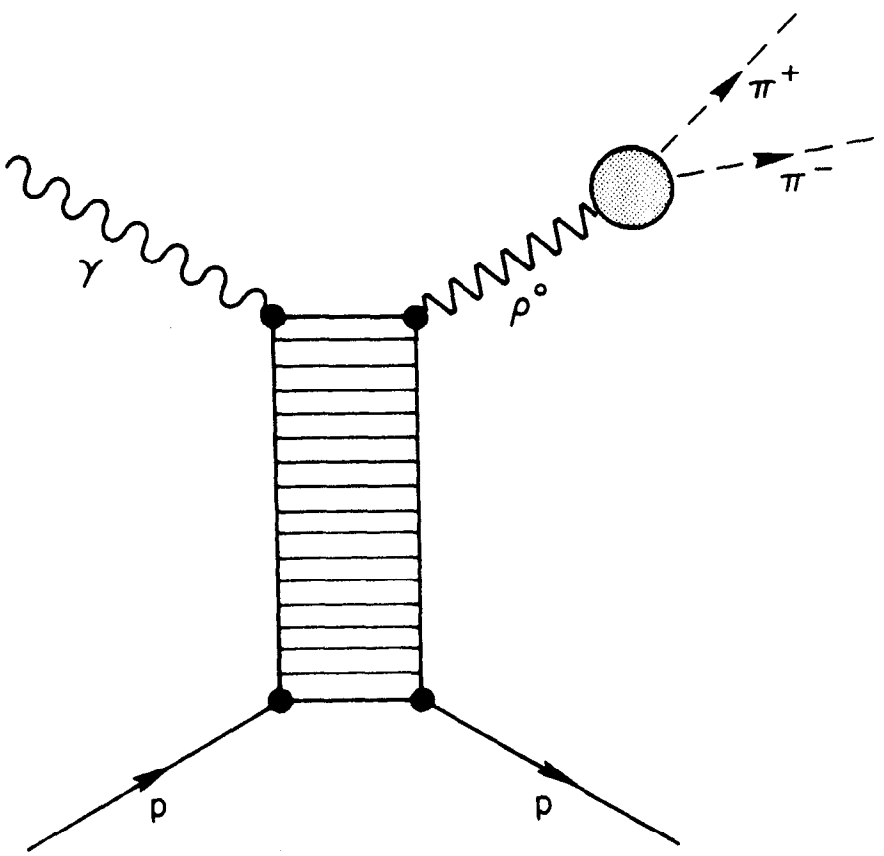


474-21-A

Fig. 25

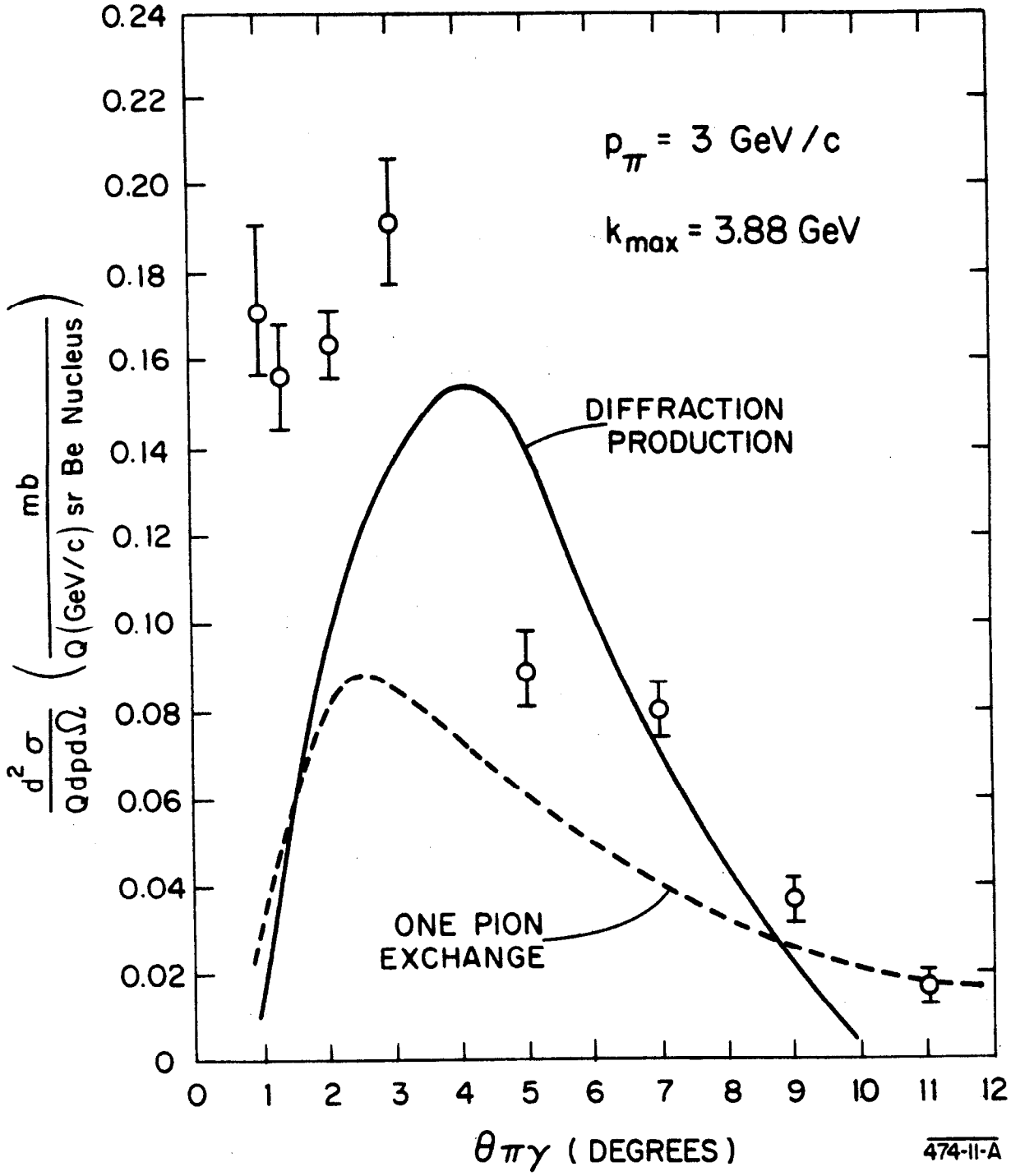
0.24
0.22
0.20
0.18
0.16
0.14
0.12
0.10
0.08
0.06
0.04
0.02
0
0 1 2 3 4 5 6 7 8 9 10 11 12
$p_\pi$ = 3 GeV/c
$k_{max}$ = 3.88 GeV
DIFFRACTION PRODUCTION
ONE PION EXCHANGE
$\frac{d^2\sigma}{Qdpd\Omega}\left(\frac{mb}{Q(GeV/c)\ sr\ Be\ Nucleus}\right)$
$\theta\pi\gamma$ ( DEGREES )
474-11-A

Fig. 26

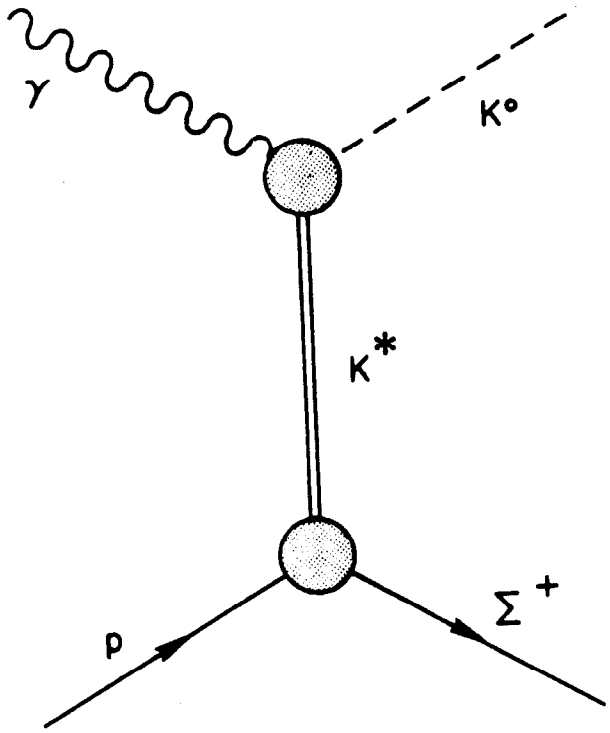


Fig. 27

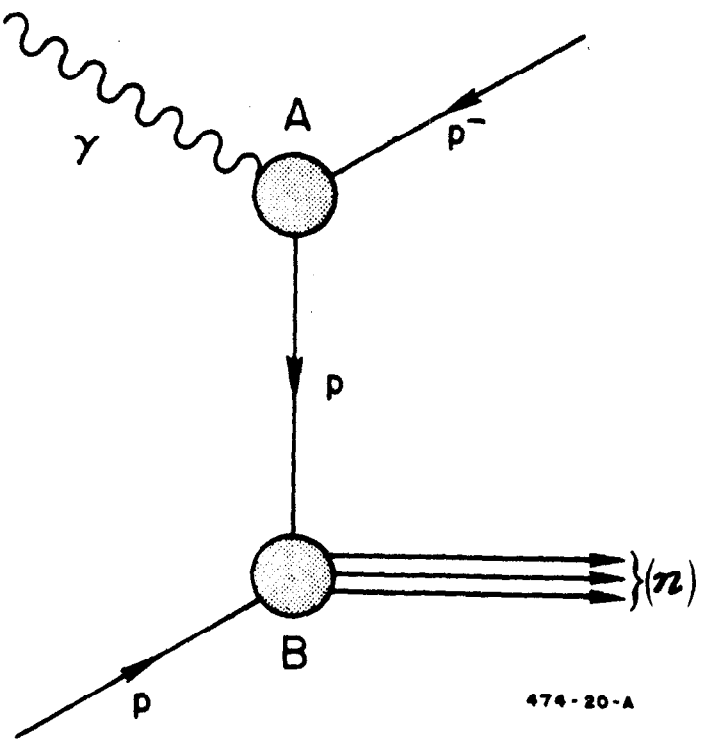


Fig. 28

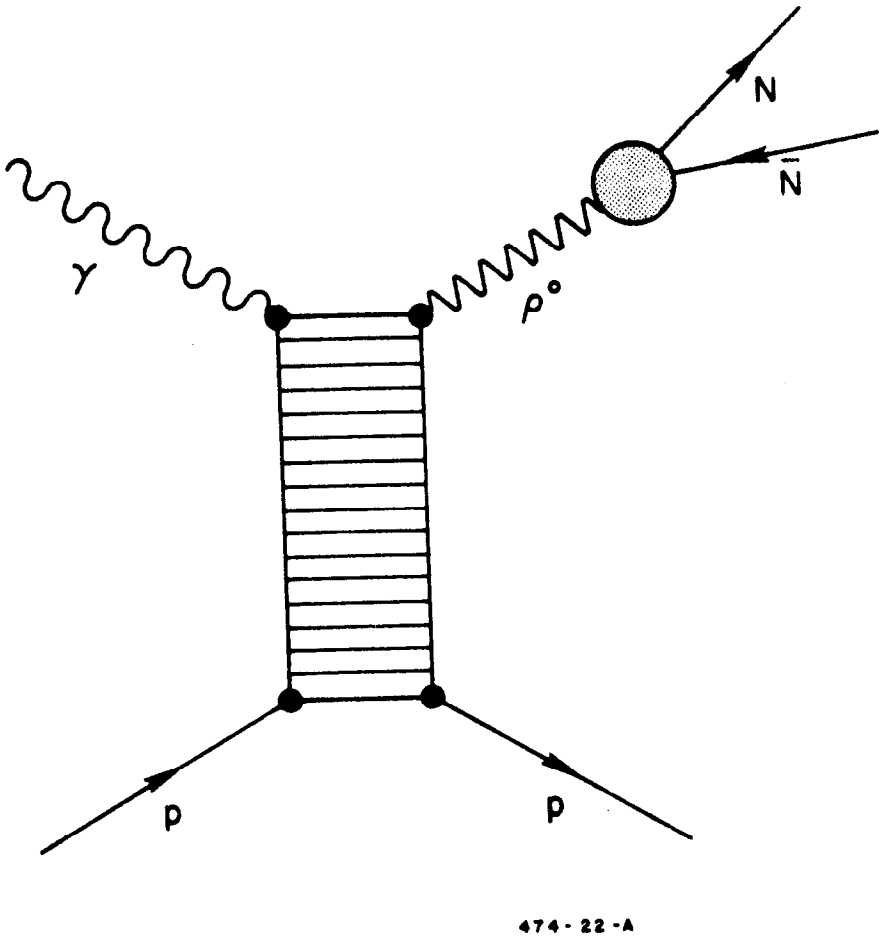


Fig. 29